WALL JET ANALYSIS FOR CIRCULATION CONTROL AERODYNAMICS, PART I: FUNDAMENTAL CFD AND TURBULENCE MODELING CONCEPTS*

S.M. Dash, B.J. York and N. Sinha
Science Applications International Corporation
Princeton, New Jersey

and

F.A. Dvorak
Analytical Methods, Inc.
Redmond, Washington

ABSTRACT

In Part I of this paper, an overview of parabolic and PNS methodology developed to treat highly curved sub and supersonic wall jets is presented. The fundamental data base to which these models have been applied is discussed in detail. The analysis of strong curvature effects has been found to require a semi-elliptic extension of the parabolic modeling to account for turbulent contributions ($\overline{v'v'}$) to the normal pressure variation, as well as an extension to the turbulence models utilized, to account for the highly enhanced mixing rates observed in situations with large convex curvature. A non-iterative, pressure-split procedure is shown to extend parabolic models to account for such normal pressure variations in an efficient manner, requiring minimal additional run time over a standard parabolic approach. Curvature corrections to a $k\varepsilon$ two-equation turbulence model are reviewed and their general applicability is assessed. For complex flows, the use of algebraic or full Reynolds stress turbulence models may be required, but the $k\varepsilon$ corrections utilized have been adequate for all fundamental cases thus far explored. For strong blowing situations, a supersonic/underexpanded wall jet structure develops with a complex multiple shock cell internal wave structure. A new PNS approach is presented to solve this problem which extends parabolic methodology via the addition of a characteristic-based wave solver. Applications of this approach to analyze the interaction of wave and turbulence processes in wall jets are presented. The present uncertainty in dealing with compressibility effects in supersonic problems

---

* Presented at Circulation Control Workshop, NASA/Ames Research Center, February 18 - 20, 1986. Work supported by David Taylor R&D Center and NASA/Ames.

is pointed out as a problem area for which no data exists. The unification of the parabolic, pressure-split and PNS wave solving capabilities into the wall jet computer code, WJET, is discussed. This code has served as a research tool for studying the effects of various parameters on wall jet structure, and includes advanced turbulence models with curvature and compressibility effects. In Part II of this paper, the steps taken towards incorporating WJET into a zonal component model for analyzing circulation control airfoils is presented.

INTRODUCTION

A zonal model (Figure 1) for the engineering analysis of circulation control airfoil performance (TRACON) was developed by Dvorak and coworkers under David Taylor R&D Center (DTRDC) support[1,2]. TRACON is comprised of separate components which analyze the external potential flow (Jameson's FL06 model), the airfoil boundary layer (Cohen and Reshotko/Green, laminar/turbulent integral models), and the wall jet (Dvorak's finite difference model[3]).

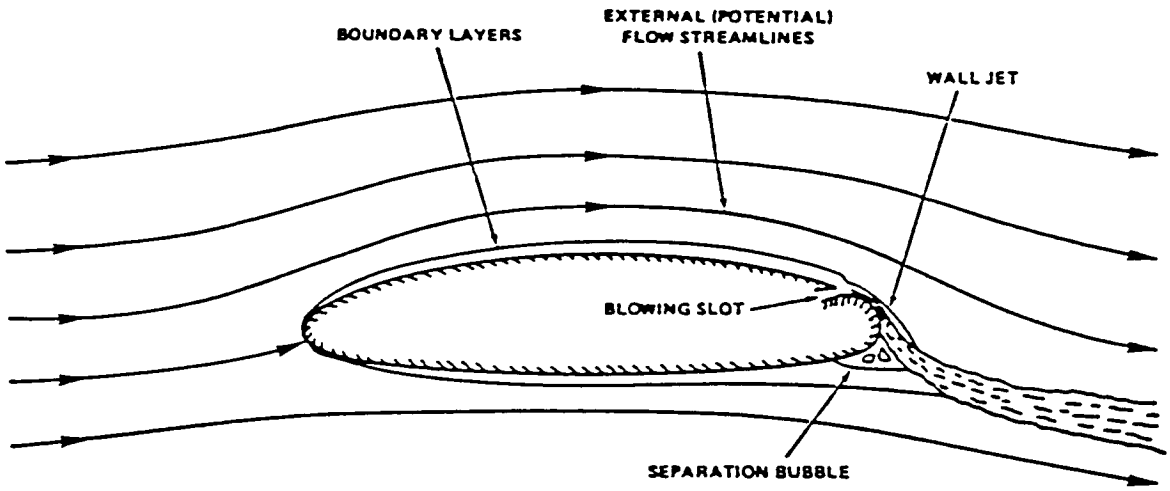

FIGURE 1. Zonal Approach for CC Airfoil Analysis.

While TRACON was demonstrated to perform quite well for a variety of cases, limitations in its ability to deal with very large curvature and/or strong blowing were encountered. These limitations were associated with the modeling assumptions in the TRACON wall jet component which include:

(1) a parabolic approach does not solve the normal momentum equation across the viscous wall jet, hence - ΔC_p is not predicted and has to be estimated from inviscid considerations;

(2) a parabolic approach which does not treat the supersonic wave/shock structure occurring in underexpanded wall jets at high rates of blowing;

(3) a weakly interactive, displacement-thickness based viscous/inviscid coupling approach which becomes inadequate for strongly interactive situations associated with large curvature and/or strong blowing; and,

(4) an algebraic eddy viscosity turbulence model which does not handle lag effects associated with significant pressure gradients.

To remedy these limitations, a new wall jet model, WJET, was developed by Dash and coworkers (under DTRDC support), which employed advanced numerical procedures and utilized a two-equation turbulence model. The first version of this model[4,5] solved the higher order parabolic curved wall jet equations utilizing a conventional implicit algorithm. This model provided for a formal solution of the viscous normal momentum equation to yield ΔC_p across the jet, and, employed a hybrid (inner VanDriest/outer kε) two-equation turbulence model with curvature correction terms. An improved version of WJET[6,7] utilized a subsonic pressure-split approach which solved the semi-elliptic coupled continuity and normal momentum equations across the jet in a non-iterative manner, and, provided for direct coupling of the wall jet with a potential external flow solver, eliminating the requirement for weakly interactive displacement thickness based coupling. The final version of WJET developed under DTRDC support[8,9], extended the parabolic/pressure-split methodology to provide PNS spatial marching capabilities in supersonic flow regions. A new implicit/explicit approach was utilized which employs an upwind finite difference representation of viscous-characteristic methodology to solve the wall jet wave field.

In concurrent work initiated in 1984 under NASA/Ames support, the methodology was formulated[10] and is now being made operational, to incorporate WJET into the TRACON code, replacing the existing wall jet component. This effort is being performed jointly by Dvorak and coworkers (at AMI) and Dash and coworkers (at SAIC). Progress towards this end is discussed in Part II of this paper[11].

In Part I of this paper, a brief overview of the features and capabilities of WJET, and, its application to various simple cases will

be discussed. WJET has been used on a stand alone basis to analyze a variety of basic wall jet data which has led to a greater understanding of the dominant influence of turbulence modeling on our ability to simulate wall jet flowfields. On highly curved convex surfaces, conventional two-equation models grossly underestimate the jet growth and the mixing that occurs, and curvature correction terms are required to properly simulate the flowfield. At supersonic velocities, free jet data indicate that compressibility effects can markedly reduce jet growth and mixing, as will be discussed. A good data base to isolate the influence of compressibility effects on wall jets is not available, which leads to some uncertainty in our ability to treat circulation control airfoil problems, but a much larger uncertainty in other higher speed problems (i.e., tangential injection problems in supersonic combustors, slot cooling problems for hypersonic vehicles, etc.).

OVERVIEW OF WJET MODEL

Mean Flow and Turbulence Model Equations

WJET solves the higher order curved boundary layer equations listed in Table 1. The equations are cast in surface-oriented s,n coordinates (Figure 2) and include a tracer species equation for ϕ (ϕ = 1 in unmixed jet, = 0 in airstream) to delineate the jet/air mixing region. A classical Boussinesq approximation is utilized to relate turbulent stress terms to mean flow gradients, with the parabolized stress terms retained listed in Table 2. Turbulence closure is achieved using the two-equation kε model with standard coefficients (C_μ = 0.09, C_1 = 1.43, C_2 = 1.92, σ_k = 1.0, σ_ε = 1.3). The turbulent transport equations for k and ε are listed in Table 3.

To extend the high Reynolds number kε turbulence model to the wall, a variety of techniques are available ranging from simple wall function approaches to the use of low Re extensions of the kε model. A review of these techniques from both a pragmatic and computational viewpoint (see ref. 5) has led to our use of a classical VanDriest mixing length formulation with damped law of the wall, as routinely employed in two layer algebraic turbulent model formulations (i.e., this comprises the inner layer component in the popular Cebeci-Smith and Baldwin-Lomax two layer formulations). Coupling between the inner (near wall) mixing length formulation and the outer kε formulation is set to occur at y^+ = 50. The values of k and ε at the matching point are determined via the requirement that the mixing length and kε turbulent viscosities match and that the turbulence is in a state of equilibrium. This yields lower boundary conditions for k and ε at the matching point. An analogous ML/kε coupling procedure has been developed by Arora et.al[12] for application to a variety of turbulent boundary layer problems. The inner/outer coupling relations are listed in Table 3 along with a schematic of the coupling procedure. Results obtained are relatively

TABLE 1 – Governing Equations

Continuity

$$\frac{\partial}{\partial s}(\rho U) + \frac{\partial}{\partial n}(h\rho V) = 0$$

Streamwise Momentum

$$\frac{\partial}{\partial s}(\rho U^2) + \frac{\partial}{\partial n}(h\rho UV) - K\rho UV + \frac{\partial P}{\partial s} =$$

$$\frac{\partial}{\partial n}\left(h\left[\tau s_n - \rho\overline{u'v'}\right]\right) - K(\tau s_n - \rho\overline{u'v'})$$

Normal Momentum

$$\frac{\partial}{\partial S}(\rho UV) + \frac{\partial}{\partial n}(h\rho V^2) + K\rho U^2 + h\frac{\partial P}{\partial n} =$$

$$\frac{\partial}{\partial n}\left(h[\tau_{nn} - \rho\overline{v'v'}]\right) + K(\tau_{ss} - \rho\overline{u'u'})$$

Energy

$$\frac{\partial}{\partial s}(\rho UH) + \frac{\partial}{\partial n}(h\rho VH) = \frac{\partial}{\partial n}\left(h\left[\frac{\mu}{P_r}\frac{\partial}{\partial n}(H)\right] - \frac{1}{2}Q^2\right.$$

$$\left. - \rho\overline{H'v'} + \overline{(\tau_{sn} + \tau'_{sn})(U + u')} + \overline{(\tau_{nn} + \tau'_{nn})(V + v')}\right)$$

Species Continuity

$$\frac{\partial}{\partial S}(\rho U\phi) + \frac{\partial}{\partial n}(h\rho V\phi) = \frac{\partial}{\partial n}\left(h\left[\frac{\mu}{P_r}\frac{\partial\phi}{\partial n}\right] - \rho\overline{\phi'v'}\right)$$

TABLE 2 – Parabolized Stress Terms

Using a Boussinesq type approximation

$$-\rho\overline{u_i'u_j'} = -\frac{2}{3}\rho k\,\delta_{ij} + \mu_t\left[\left(\frac{\partial U_i}{\partial X_j} + \frac{\partial U_j}{\partial X_i}\right) - \frac{2}{3}\,\mathrm{div}\,\bar{V}\right]$$

(where the turbulent kinetic energy $k = u_i'u_i'/2$), the parabolized turbulent stress terms in curvilinear surface-oriented coordinates take the following form:

$$-\rho\overline{u'v'} = \mu_t\left(\frac{\partial U}{\partial n} + \frac{KU}{h}\right)$$

$$-\rho\overline{u'u'} = -\frac{2}{3}\rho k - \frac{\mu_t}{h}\left[2KV + \frac{2}{3}\frac{\partial}{\partial n}(hV)\right]$$

$$-\rho\overline{v'v'} = -\frac{2}{3}\rho k + \mu_t\left[2\frac{\partial v}{\partial n} - \frac{2}{3h}\frac{\partial}{\partial n}(hV)\right]$$

The turbulent transport of a scalar variable, α, is expressed by

$$-\rho\overline{\alpha'v'} = \frac{\mu_t}{\sigma_\alpha}\frac{\partial\alpha}{\partial n}$$

For both H and ϕ, σ_α is taken to be the turbulent Prandtl number, P_{r_t}.

TABLE 3 – Turbulent Transport Equations and Inner (ML) / Outer (kε) Coupling

$$\rho U \frac{\partial k}{\partial s} + h\rho V \frac{\partial k}{\partial n} = \frac{\partial}{\partial n}\left[\frac{h\mu_{eff}}{\sigma_k}\frac{\partial k}{\partial n}\right] + \underline{P} - \rho\varepsilon$$

$$\rho U \frac{\partial \varepsilon}{\partial s} + h\rho V \frac{\partial \varepsilon}{\partial n} = \frac{\partial}{\partial n}\left[\frac{h\mu_{eff}}{\sigma_\varepsilon}\frac{\partial \varepsilon}{\partial n}\right] + \frac{\varepsilon}{k}\left(C_1\underline{P} - C_2\rho\varepsilon\right)$$

where the production term, $\underline{P}$, is given by

$$\underline{P} = \mu_t \left(\frac{\partial U}{\partial n} + \frac{KU}{h}\right)^2$$

$$k_{I*} = L^2_{I*} \left|\partial u/\partial n\right|^2_{I*}/C_\mu^{1/2}$$

$$\varepsilon_{I*} = C_\mu^{3/4} k_{I*}^{3/2}/L_{I*}$$

$$\mu_t = \rho L^2 \left|\frac{\partial u}{\partial n}\right|$$

$$L = \kappa n \left[1 - \exp(y^+/A)\right]$$

$\kappa = .41$ and $A = 27$

$$y^+ = n \tau_s^{1/2} \rho^{1/2}/\mu_l$$

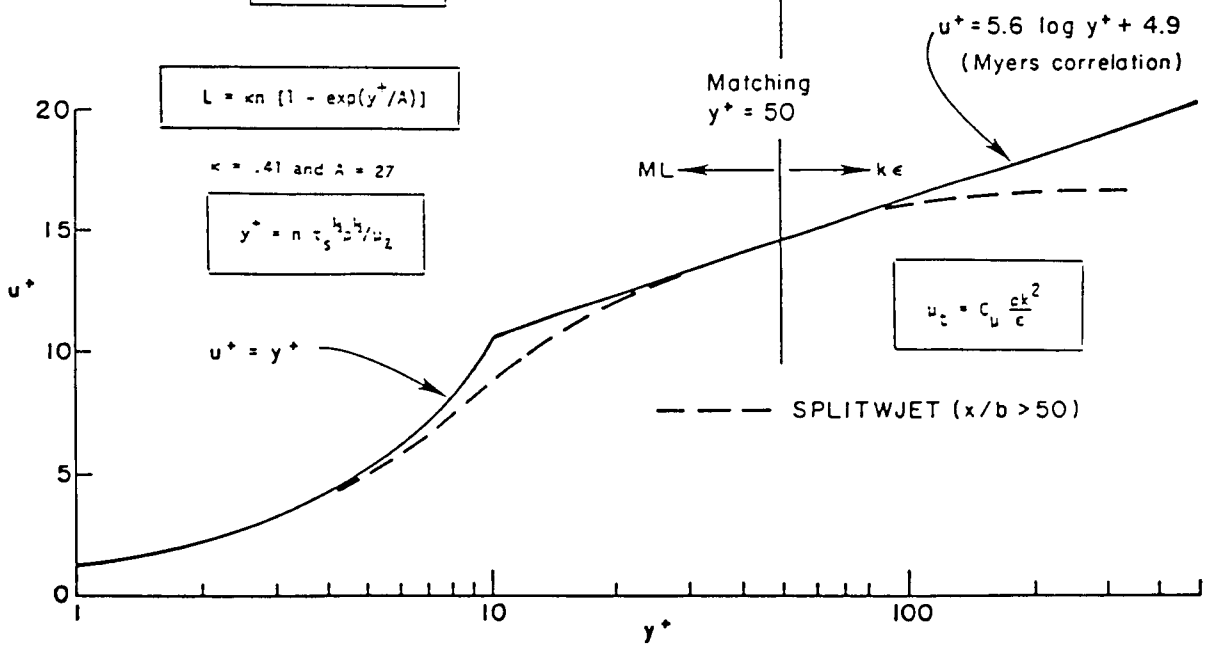

insensitive to the value of y^+ utilized for the coupling as long as it nominally remains in the log region (viz., $20 \sim y^+ \sim 100$).

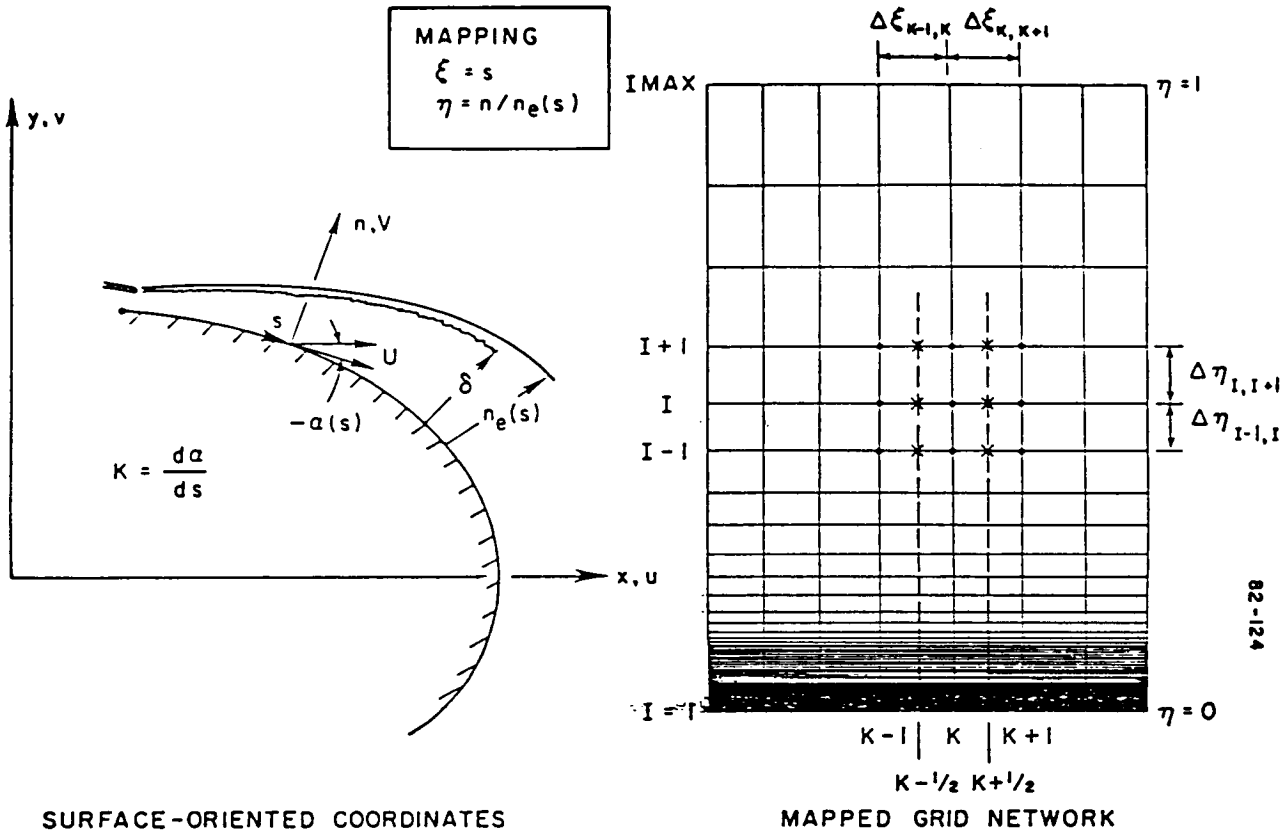

FIGURE 2. Surface-Oriented Grid Nomenclature and Mapped/Stretched Grid Utilized.

While both the mean flow and turbulence model equations contain a number of curvature terms arising from the transformation to curvilinear, surface-oriented coordinates, numerous investigators have demonstrated that additional, curvature corrections terms are required to account for the strong effects of curvature on wall jet turbulence structure. The analogy drawn by Bradshaw[13] between curvature and buoyancy has been utilized by most investigators as the basis for heuristic corrections to algebraic or two-equation turbulence models. Defining the curvature parameter, $s = -KU/(\partial U/\partial n)$, a curvature correction to the ML formulation is given by:

$$L = \frac{L_o(1-\alpha s)}{(1-s)} \tag{1}$$

where L_o is the planar length scale value, while α is a constant, $(5 < \alpha < 10)^o$. This treatment has been implemented for curved wall jets by Foloyan and Whitelaw[14] who utilized a complete (inner/outer) mixing length formulation. For the present near wall use of the mixing length formulation, this correction will only be required in situations with very large curvature. For problems with small to moderate curvature, the near wall region correction to L_o is negligible.

Launder and coworkers[15] have developed a curvature correction for the $k\varepsilon$ model which utilizes a single empirical coefficient, C_c. The curvature correction is proportional to a Richardson number, Ri_c, based on the turbulence time scale. In their formulation, the local Richardson number is given by:

$$Ri = -KU \left(\frac{k}{\varepsilon}\right)^2 \frac{\partial U}{\partial n} \tag{2}$$

and the C_2 coefficient of the ε equation is modified as follows:

$$C_2 = 1.92\ (1 - C_c Ri) \tag{3}$$

Values of C_c of about 0.2 have yielded optimal predictions for a variety of curved boundary layer flows as described in reference 15.

An analogous type of curvature correction for the $k\varepsilon$ model has been developed by Hah and Lakshminarayana at Penn State[16]. They have modified the C_1 coefficient of the ε equation as follows:

$$C_1 = 1.43\ (1 + C_c Ri) \tag{4}$$

We have implemented the Penn State correction using the Launder definition of Ri in our model.

At supersonic wall jet velocities, a compressibility correction analogous to that of Dash, et.al.[17] for free shear layers, may be required. Here, a factor whose magnitude varies from 1.00 at M = 1 to 0.25 for large Mach numbers is used to multiply the C_μ coefficient of the $k\varepsilon$ model. This correction factor is an empirical expression derived from experimental free shear layer observations and is calculated as follows:

$$f_{cc} = 0.25 + 0.75/\{1.0+\exp[24.73(M_\tau-0.2)]\} \quad (5)$$

where M_τ is the Mach number characterizing the fluctuating velocity field, (e.g., $k^{1/2}$ divided by the local speed of sound).

For free shear layers, M_τ is evaluated at the position of maximum k at each station. Its adaptation to supersonic wall jets would entail utilizing the value of k at the position of maximum velocity and incorporating a transverse dependence to smoothly reduce the correction in the 'boundary layer' portion of the wall jet (below the peak velocity point). Data exhibiting the dependence of mixing on the wall jet Mach number is not presently available to derive a correlation analogous to that of equation (5) for wall jet flows.

NUMERICAL PROCEDURES

Splitting of Solution into Parabolic and Elliptic/Hyperbolic Components

The approach taken in WJET involves combining:

(1) a parabolic solution of the streamwise momentum, energy, species parameter, and turbulence model equations with the streamwise pressure gradient term, $\partial P/\partial s$ (s,n) specified - this solution yields the variation of U, H, ϕ, k and ε;

(2) an elliptic/pressure-split solution of the coupled continuity and normal momentum equations in subsonic regions which yields the variation of pressure and normal velocity across the wall jet; and,

(3) a hyperbolic/upwind characteristic-based solution of the coupled continuity and normal momentum equations in supersonic regions which yields the local pressure and flow angle.

These three solution procedures are unified in the WJET code to provide generalized spatial marching capabilities for a broad category of wall jet problems.

Parabolic Analysis

The WJET parabolic algorithm integrates the U momentum, H, ϕ, k and ε equations (Table 1) in mapped rectangular coordinates (Figure 2). The mapped, vectorized equations take the form:

$$\rho U \frac{\partial f}{\partial \xi} + b(hcV - \frac{a}{b}\rho U)\frac{\partial f}{\partial \eta} = b^2 \frac{\partial}{\partial \eta}\left[\frac{h\mu_{eff}}{\sigma_f}\frac{\partial f}{\partial \eta}\right] + g_f \qquad (6)$$

where:

$$f = [\, U,\ H,\ \phi,\ k \text{ and } \varepsilon \,]^T$$

a and b are mapping parameters, and g_f is the source term. The equations are spatially integrated using an upwind/implicit algorithm. A fixed number of grid points are distributed between the wall ($\eta = 0$) and outer viscous boundary ($\eta = 1$) whose growth is obtained via adaptive methodology keyed to the edge gradients. The distribution of grid points, $\eta(I)$, remains invariant throughout the calculation and the stretching utilized can be arbitrarily stipulated, or specified using built in grid distribution parameters. The equations are solved in an uncoupled manner (the source terms are solved explicitly) and the difference equations then take standard tridiagonal form. Complete details of the parabolic algorithm are available in references 4 and 5.

Pressure-Split Subsonic Cross-Flow Analysis

To analyze subsonic wall jets with large curvature, a pressure-splitting approach analogous to that of Bradshaw and coworkers[18,19] is utilized. In the pressure-splitting procedure, the global pressure field, $P^*(s,n)$, utilized to evaluate $\partial P/\partial s$ in the streamwise momentum equation, must be stipulated. This is initially estimated to be the inviscid pressure field prevailing in the region occupied by the wall jet. In the pressure-splitting approximation, the parabolic equations are integrated with $\partial P/\partial s$ obtained from $P^*(s,n)$. However, the pressure field is revised in the course of the spatial integration by solving the coupled continuity and normal momentum equations across the jet with the inviscid pressure prevailing at the edge of the jet serving as an outer boundary condition. Global convergence in regions of strong curvature is obtained by repeating the calculation with the revised pressure field until the imposed and upgraded pressures are effectively the same.

By manipulations described in references 6 and 7, the continuity equation (in mapped coordinates) can be written in terms of pressure, P, and normal velocity, v, yielding:

$$\gamma\,(a+\bar{V}/U)\frac{\partial P}{\partial \eta} + (\gamma-1)\,\rho\, V \frac{\partial V}{\partial \xi} + \left[\frac{\rho b h C^2}{U} + (\gamma-1)\frac{\rho V \bar{V}}{U}\right]\frac{\partial V}{\partial \eta} = g_p \qquad (7)$$

where the source term, g_p, is listed below:

$$g_p = \rho b C^2 \frac{\partial}{\partial \eta}\left(\frac{a}{b}\right) + K \rho C^2 \frac{V}{U} - \left[\frac{\rho C^2}{U} + (\gamma-1)\rho U\right] \frac{\partial U}{\partial \xi}$$

$$+\left[\frac{\rho a C^2}{U} - (\gamma-1)\rho \tilde{V}\right] \frac{\partial U}{\partial \eta} + (\gamma-1)\rho \left[\frac{\partial H}{\partial \xi} + \frac{\tilde{V}}{U}\frac{\partial H}{\partial \eta}\right]$$

$$- \gamma \frac{\partial P^*}{\partial s} + \frac{\rho C^2}{b}\frac{\partial b}{\partial \xi}$$

Note that g_p contains partial derivatives of U and H (which are evaluated a priori as part of the parabolic solution) and also contains the prescribed streamwise pressure gradient term. The normal momentum equation given below (g_v represents turbulent stress terms - see Table 2):

$$\rho U \frac{\partial V}{\partial \xi} + \rho \tilde{V} \frac{\partial V}{\partial \eta} + bh \frac{\partial P}{\partial \eta} + K \rho U^2 = g_v \qquad (8)$$

is solved with the continuity equation in a coupled manner to yield the variation of P and v across the wall jet (see references 6 and 7 for details).

Figure 3 illustrates results obtained using this pressure-split approach to analyze the simple case of a curved wall jet issuing into still air. Shown are the wall jet geometry, maximum velocity decay (contrasted to the variation for a flat wall), induced entrainment (also contrasted to the flat wall variation), surface pressure variation (utilizing viscous and inviscid forms of the normal momentum equation) and a decomposition of terms in the normal momentum equations showing their individual contributions to ΔC_p across the wall jet. Note that the very significant contribution of turbulent stress terms (specifically $\overline{v'v'}$) to the ΔC_p across the jet. Complete details of this case are provided in references 6 and 7.

Upwind Characteristic-Based Supersonic Wave Solver Analysis

To analyze supersonic regions of underexpanded wall jets, a characteristic-based procedure is employed to locally evaluate the wave field (e.g., to obtain pressures and flow angles at each grid point). The approach taken involves a 'modern' formulation of viscous-characteristic methodology originally developed about 20 years ago[20,21]. The viscous-characteristics approach involves manipulating the continuity and normal momentum equations to obtain characteristic relations of the form:

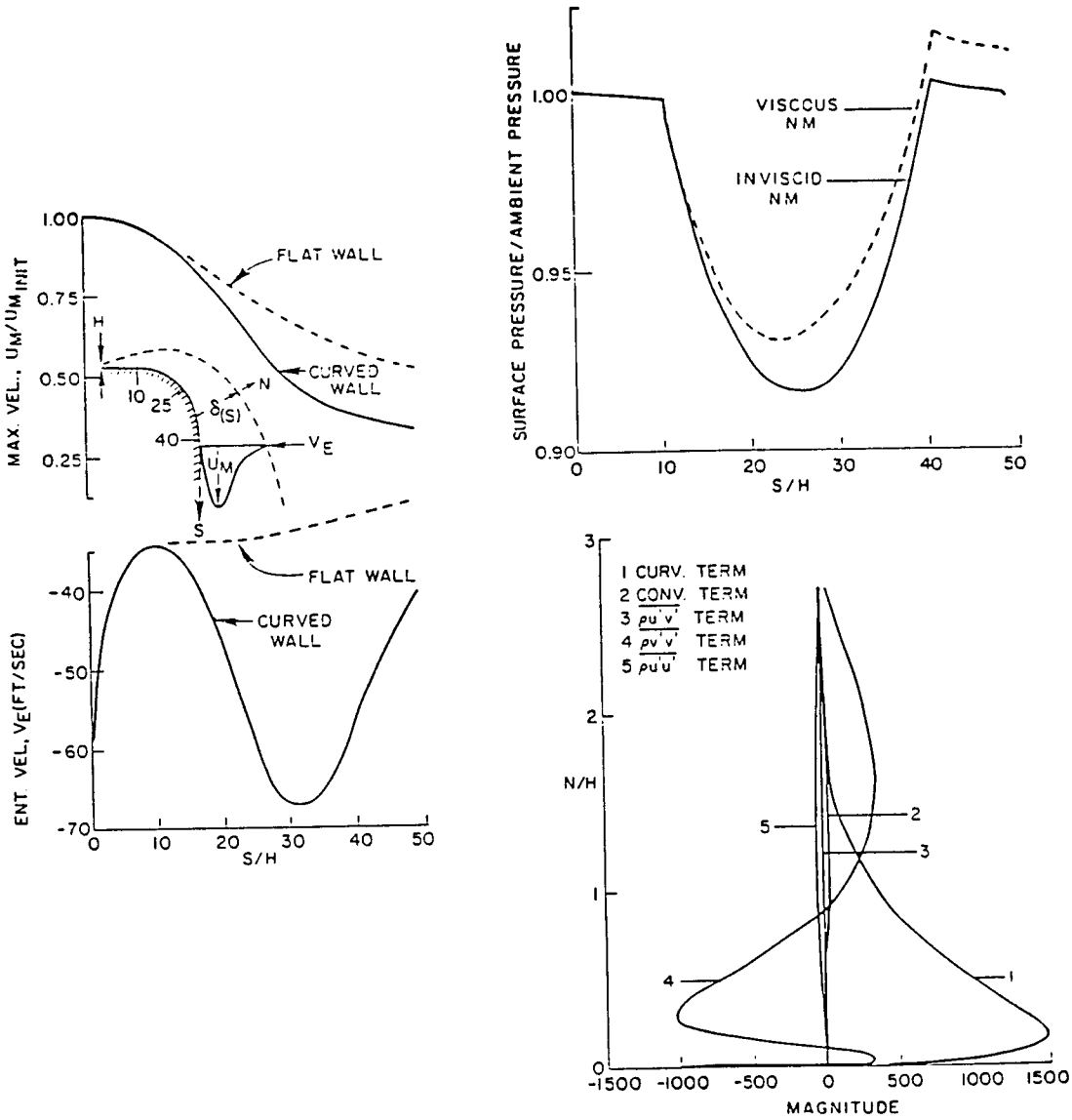

FIGURE 3. Pressure-Split Analysis of Curved Wall Jet Issuing into Still Air.

$$\frac{\sin\mu\cos\mu}{\gamma}\,d\ln p \pm d\theta = \frac{-J\sin\theta\sin\mu}{r}\,d\lambda^{\pm} + \tilde{F}^{\pm}d\lambda^{\pm} \qquad (9)$$

where the source term, $\tilde{F}$, contains the viscous stress terms, and diffusive transport terms, appearing on the r.h.s. of the streamwise momentum (F_u), normal momentum (F_v), and energy (F_H) equations. The source term, $\tilde{F}$, is given by:

$$\tilde{F}^{\pm} = A(F_u+F_v) + BF_H \qquad (10)$$

where:

$$A = -[(1+(\gamma-1)M^2)\sin\mu\cos\theta \pm \cos\mu\sin\theta]/(\gamma PM^2)$$

and:

$$B = -(\gamma-1)\sin\mu/(\gamma PQ)$$

The nomenclature for the characteristic equations is exhibited in Figure 4.

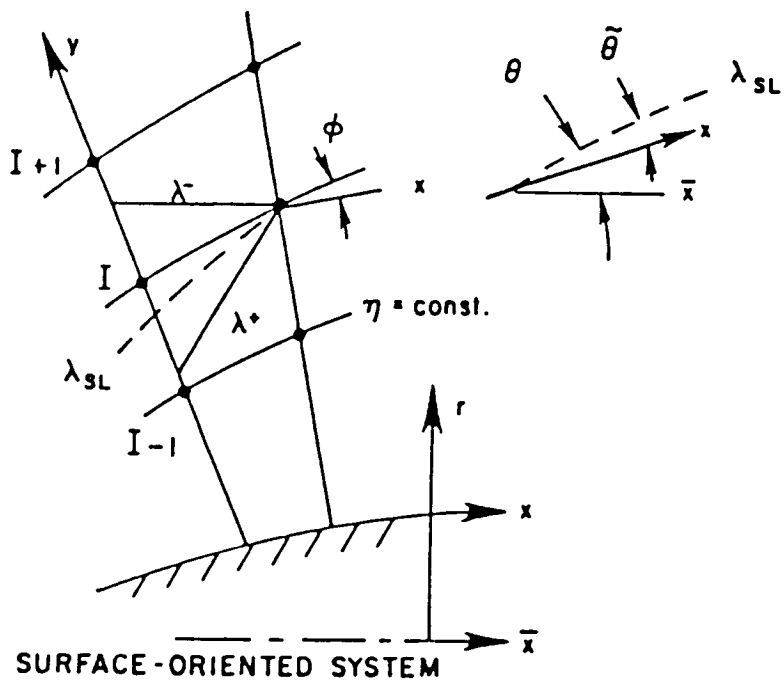

FIGURE 4. Nomenclature for Characteristic Equations.

In earlier applications of this approach, inverse characteristic methodology was utilized which was extremely cumbersome. The new approach developed[8,9] involves representing total derivatives along characteristics as a combination of streamwise and normal partial derivatives in a mapped (ξ,η) computational space. The normal derivatives are evaluated at the known station using an upwind formulation keyed to the λ^- characteristic direction. With the manipulations described in references 8 and 9, the pressure at grid point I at $\xi + \Delta\xi$ can be evaluated as a function of the pressures and flow angles at grid points I-1, I and I+1 at station ξ. This new formulation is summarized in Table 4. In present applications of WJET, the coupled parabolic/hyperbolic solution is performed in the following three step sequence:

(1) Prediction of wave field (P,θ) at $\xi + \Delta\xi$ solving pressure equation and comparable flow angle equation (Table 4) using coefficients evaluated at ξ at characteristic intersection points, and, viscous terms, F_u, F_v and F_H evaluated at ξ at grid points I.

(2) Solution of parabolic system of equations (eq. 6) yielding f at $\xi + \Delta\xi$. Pressure gradients 'prescribed' in accordance with wave field solution of step (1).

(3) Correction of wave field at $\xi + \Delta\xi$ using coefficients averaged along characteristics and, values of F_u, F_v and F_H which are evaluated at $\xi + \Delta\xi$ if the parabolic algorithm of Step (2) is fully implicit; or, are averaged across the integration step if a Crank-Nicolson parabolic procedure is utilized.

The formulation was first checked out in the inviscid limit for weak shock-capturing capabilities and produced results comparable to those of the SCIPPY code (explicit MacCormack algorithm) as exhibited in Figure 5 (see ref. 8 for details). For strong shock waves in inviscid regions, artificial viscosity must be introduced to stabilize the shock calculation and to generate entropy. The approach taken parallels that utilized in Beam and Warming based PNS algorithms and is described in reference 22.

The wave solver formulation was then checked out for supersonic viscous/inviscid jet interaction problems by comparing WJET predictions with those of the well tested SCIPVIS PNS jet mixing model (see refs. 23 - 26). These comparisons are described in references 8, 22 and 27. A typical comparison is exhibited in Figure 6 showing the interaction of an expansion fan with a free turbulent shear layer.

TABLE 4 - Characteristic-Based Upwind Formulation for Determining Local Pressures in Supersonic Flow Regions

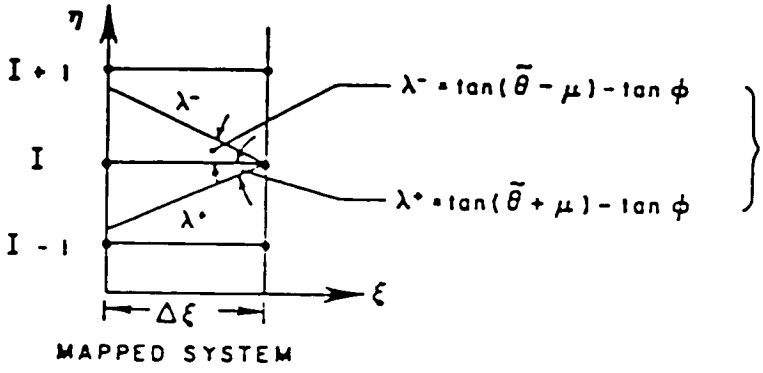

$$\left.\frac{d}{dx}\right|_{\lambda^{\pm}} = \frac{\partial}{\partial \xi} + \lambda^{\pm}\frac{\partial}{\partial \eta}$$

Pressure-Wave Solver Equations in Mapped Coordinates

$$\left.\frac{d}{dx}\right|_{\lambda^{\pm}} = \frac{\partial}{\partial \xi} + \lambda^{\pm}\frac{\partial}{\partial \eta}$$

$$C\left[\frac{\partial \ln p}{\partial \xi} + \lambda^{\pm} b \frac{\partial \ln p}{\partial \eta}\right] \pm \left[\frac{\partial \theta}{\partial \xi} + \lambda^{\pm} b \frac{\partial \theta}{\partial \eta}\right] = F^{\pm}$$

$$C = \frac{\sin u \cos u}{\gamma}$$

$$F^{\pm} = \tilde{F}^{\pm}/\cos(\theta \pm \mu)$$

$$\bar{p}_I = a_1 p_{I+1} + a_2 p_I + a_3 p_{I-1} + a_4 \theta_{I+1} + a_5 \theta_I + a_6 \theta_{I-1} + \bar{F}_I$$

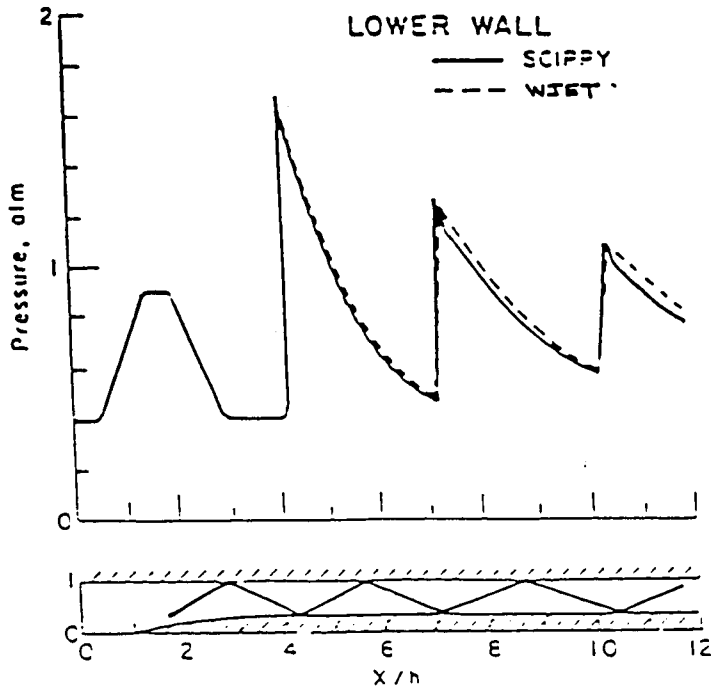

FIGURE 5. Comparison of WJET Wave Solver and SCIPPY Shock-Capturing Predictions.

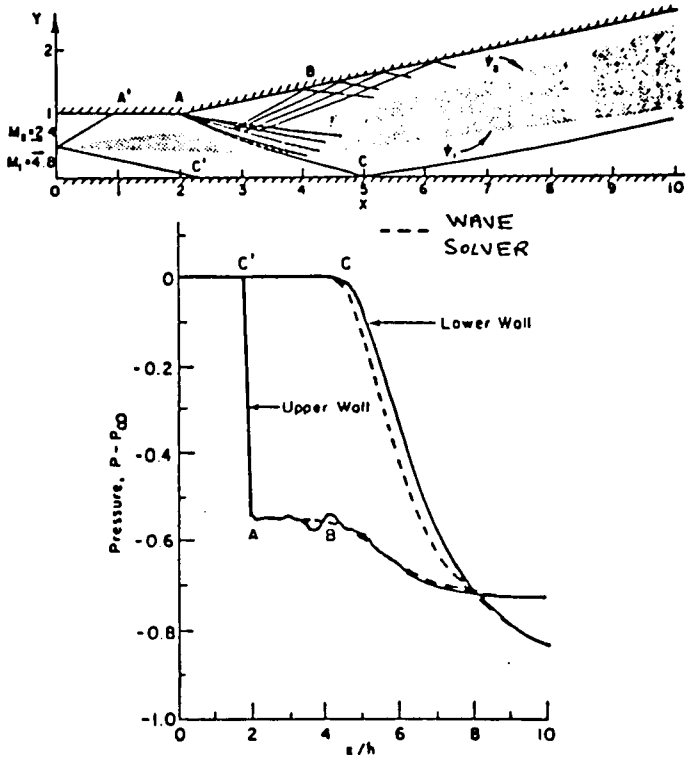

FIGURE 6. Comparison of Wave/Shear Layer Interactions; SCIPVIS (——) Versus Wave Solver (----) Predictions.

Unified Parabolic/Pressure-Split/Wave Solver Model

The WJET code unifies the three solution procedures described above, providing for PNS-based spatial marching capabilities comparable to those developed for free jet problems (see Table 5 and refs. 23 - 26). Referring to Figure 7, the wall jet problem is more complicated than the corresponding free jet problem since subsonic/supersonic coupling is required at both inner (I_1^*) and outer (I_2^*) sonic lines.

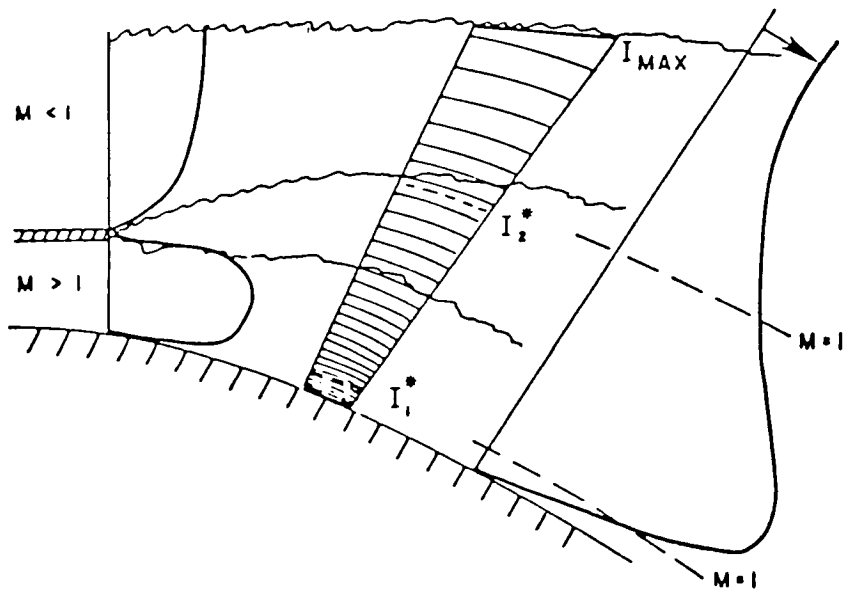

FIGURE 7. Flow Segmentation for Underexpanded Wall Jet Problem.

For free jets, a data base exists for underexpanded problems (see, e.g., ref. 28) which has been utilized for detailed verification[23,25,26]. Figure 8 exhibits predicted wave/mixing layer structure of mildly underexpanded Mach 2 free jet issuing into still air, and, comparisons of predicted and measured turbulent intensities, u'u' (u'u' = 2gk where k is the predicted turbulent kinetic energy and g is an isotropy parameter used to related k to u'u'; g = 2/3 represents the isotropic situation and appears to best correlate with the measurements). Figure 9 exhibits comparisons of the predicted pressure variations (axis and off axis) with the data. The comparisons exhibited here (and the additional comparisons described in refs. 23, 25, 26 and 28) are quite good and were obtained using the kW turbulence model.

TABLE 5 – Aspects of PNS Approach for Free Jets

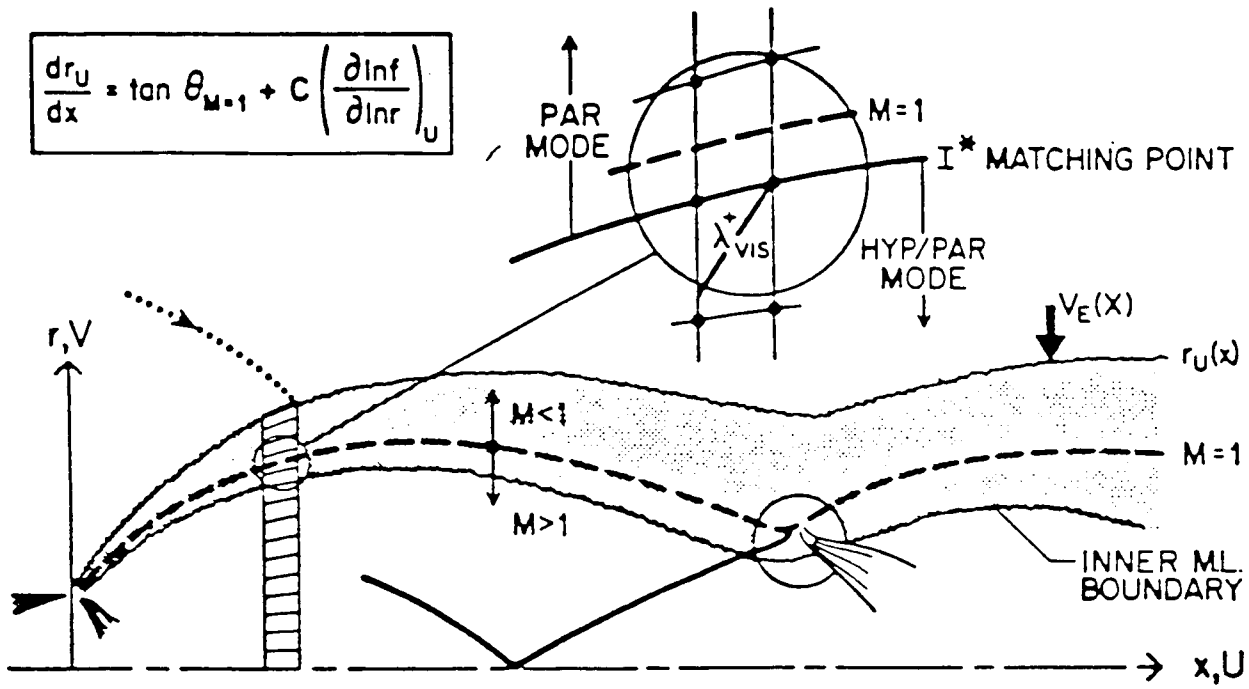

- Shock-Capturing PNS Solution in Supersonic Mixing Regions
- Pressure-Split Approximation in Subsonic Mixing Regions
- Subsonic/Supersonic Coupling at Viscous Sonic Lines
- Use of Compressibility Corrected Two-Equation Turbulence Models
- Solution in Mapped Coordinates Encompassing Viscous/ Inviscid Jet
- Direct-Coupling with External Flow Solution at Outer Viscous Boundary

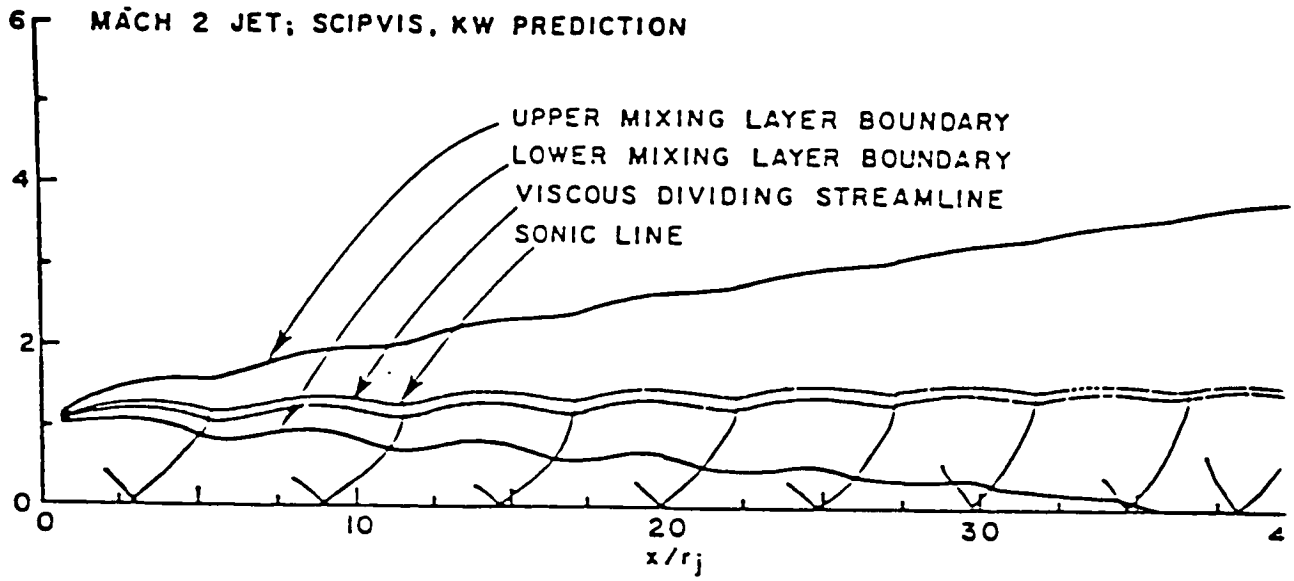

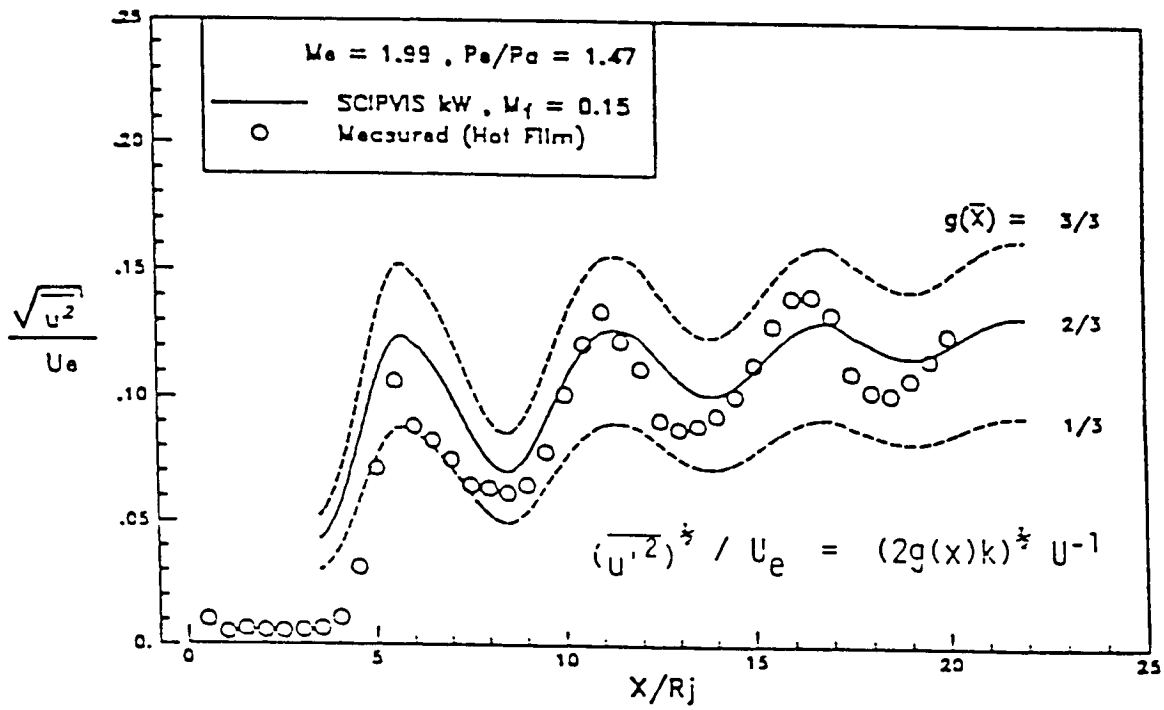

FIGURE 8. Predicted Wave/Mixing Layer Structure of Underexpanded Mach 2 Free Jet and Comparisons of Turbulent Intensity with Data.

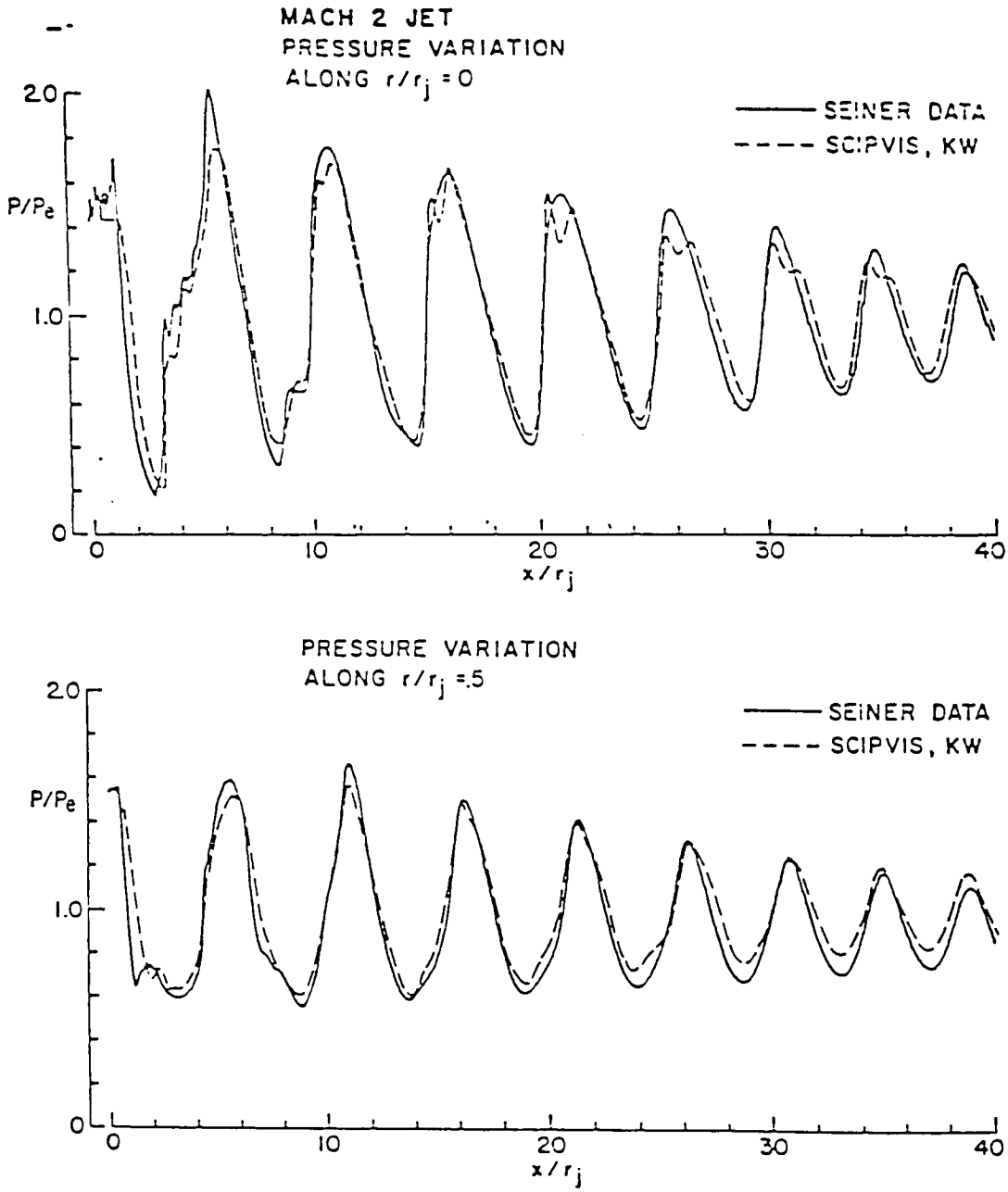

FIGURE 9. Comparison of Predicted and Measured Streamwise Pressure Variations; kW Model Solution.

Results with a standard $k\varepsilon$ model exhibit too fast a rate of mixing as would be expected from earlier comparisons with simple (balanced pressure) shear layer and jet data at supersonic velocities. The issue of compressibility effects in supersonic free turbulent shear layers has been addressed from a pragmatic viewpoint (see refs. 17, 29 - 31) and two-equation turbulence models are now available[32] which can adequately analyze the rather broad base of 'fundamental' high speed free shear layer/jet data and also, some non-fundamental situations with significant wave structure, as exhibited above.

Preliminary calculations made with WJET for an underexpanded curved wall jet are exhibited in Figures 10 through 12. Figure 10 exhibits the overall geometry and predicted streamwise variations of principal jet surfaces (viz., inner/outer shear layer boundaries where ϕ = 0.95/0.05, jet half radius, outer sonic line, and outer/adaptive computational boundary) in physical (x,y) and surface-oriented coordinates. Figure 11 exhibits the variation of wall pressure and skin friction coefficient - note the rapid response of skin friction to the wave field (the details of the interactive procedure for analyzing the near wall subsonic portion of the wall jet are described in refs. 8 and 9). Figure 12 exhibits predicted profiles of pressure and Mach number across the jet. Also shown is the normal grid distribution which is highly stretched in the near wall region (viz., from wall to position of velocity maximum - typically, y^+ of second grid point is ~ 1 and the same number of grid points span the near wall region and the outer region), and, equally spaced in the outer region (from maximum velocity position to outer boundary).

Unfortunately, adequate data to validate underexpanded wall jet solutions and thus resolve turbulence issues regarding compressibility effects, etc., is not presently available, and, hence, no such comparisons with data are exhibited in this article. The high speed wall jet data base available has recently been reviewed (under programs geared towards high speed film cooling and tangential injection in supersonic combustors). No data has been identified as suitable for turbulence model validation due to lack of key measurements (e.g., detailed initial profiles, turbulence levels, etc.). These issues are described in references 33 and 34.

Coupling Procedures for Wall Jet and External Potential Flow

To incorporate the wall jet code in a zonal approach for analyzing circulation control airfoils, a variety of coupling techniques were reviewed as discussed in references 4 and 5. Figure 13 schematizes coupling procedures available for subsonic wall jets. The displacement-thickness coupling approach overlaps the inviscid and viscous solutions and utilizes standard boundary layer concepts which break down for thick, highly curved viscous layers where the normal pressure variation is significant. The direct pressure-split coupling approach introduced

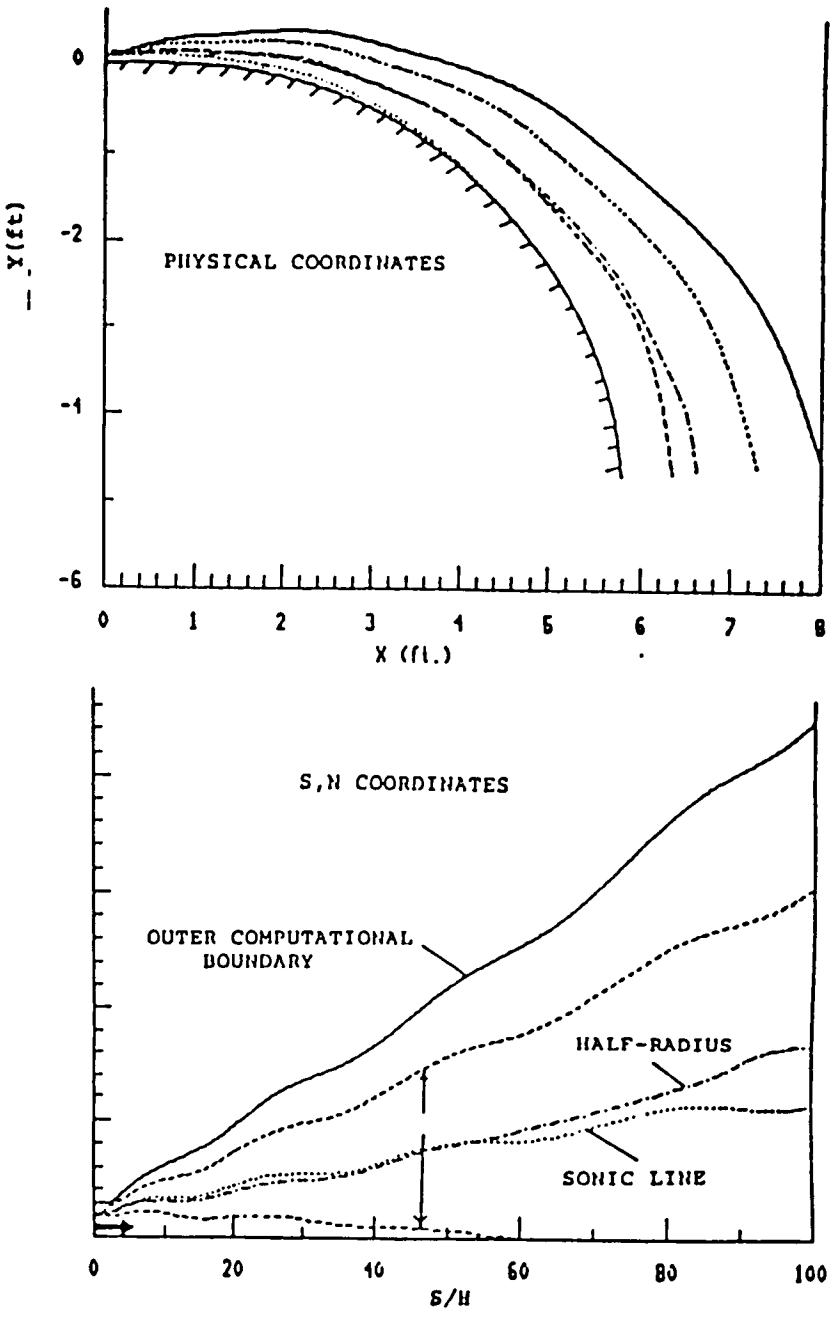

FIGURE 10. Predicted Features of Curved Underexpanded Wall Jet Issuing into Still Air.

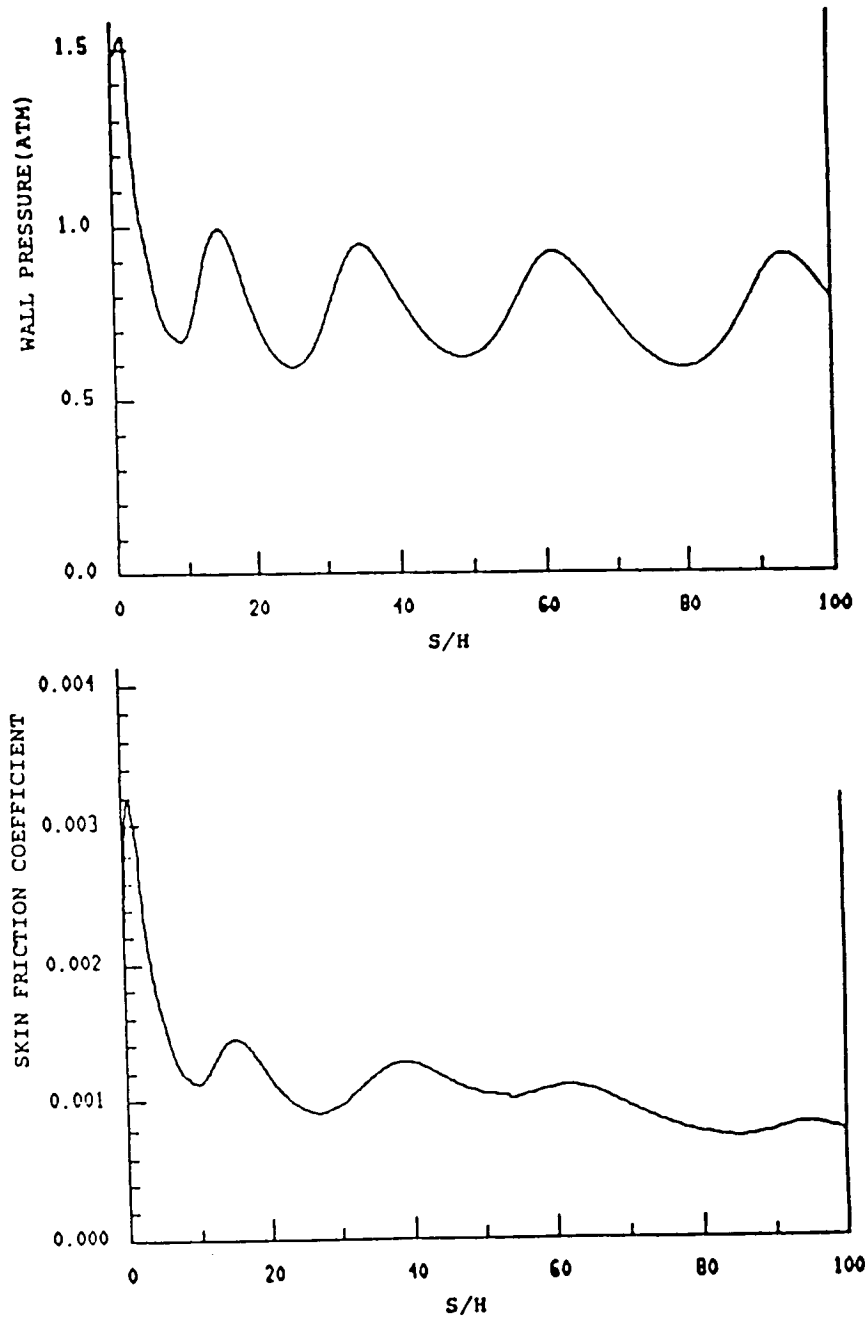

FIGURE 11. Predicted Wall Pressure and Skin Friction Variation for Curved Underexpanded Wall Jet Issuing into Still Air.

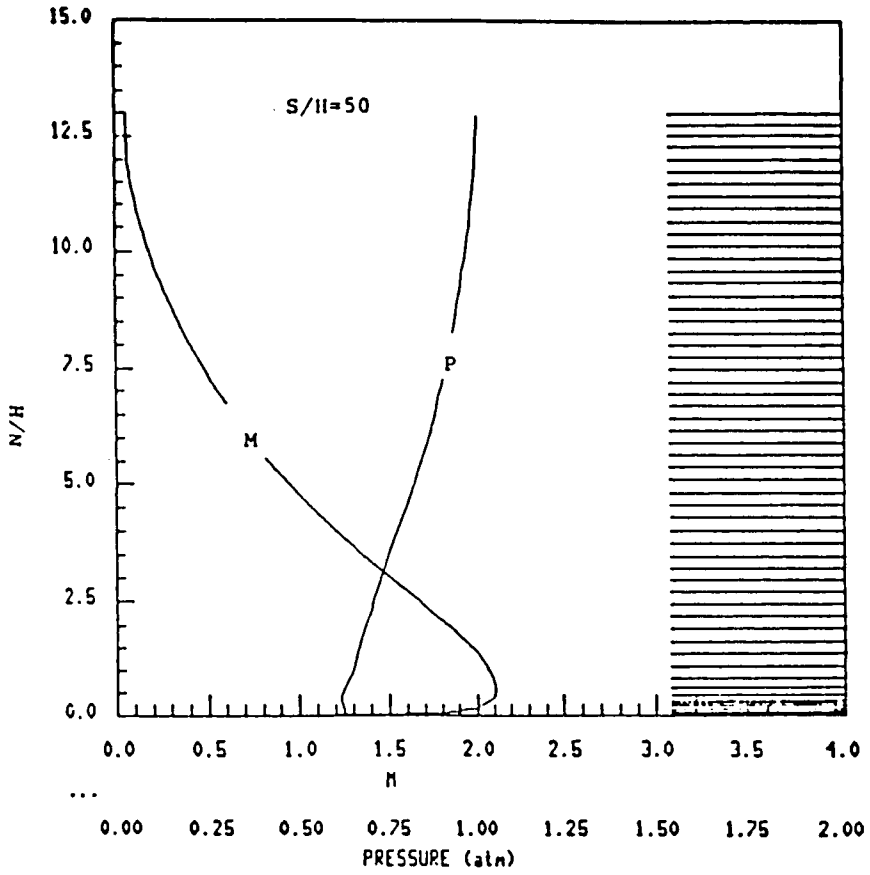

FIGURE 12. Pressure and Mach Number Profiles at Position Fifty Slot Heights Downstream of Slot.

by Bradshaw and coworkers[18,19] couples the viscous and inviscid solutions at the jet viscous boundary, and the pressure field within the jet is determined by the pressure-splitting methodology described above which directly accounts for the contribution of stress/diffusive terms. Details of this coupling methodology for wall jets are described in references 6 and 7. Velocity-split coupling also directly involves a complete overlap of viscous and inviscid solutions, but here, the coupling is intimate and can account for separated flow regions. Applications of this approach to nozzle afterbody problems have been quite successful (see refs. 37 and 38) and results comparable to full NS results have been achieved in a fraction of the run time.

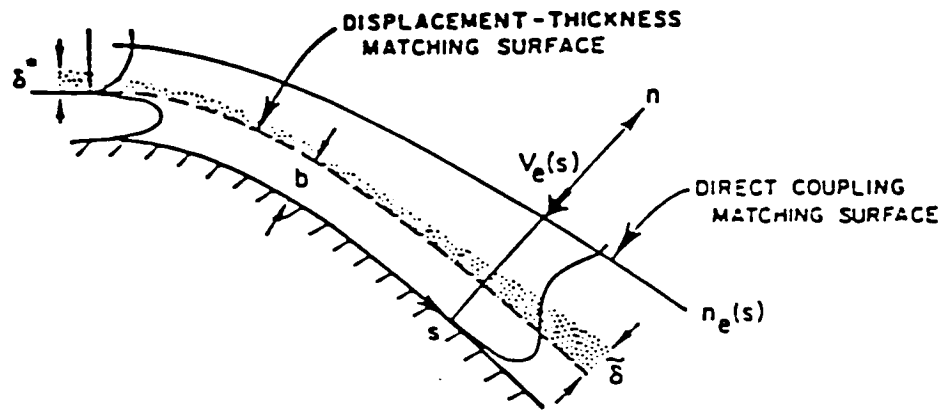

• DISPLACEMENT-THICKNESS COUPLING

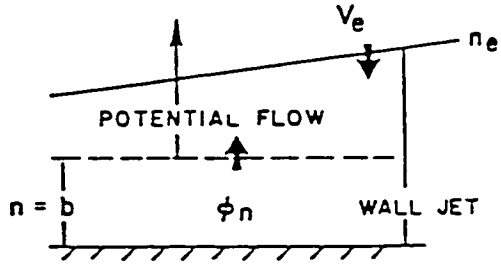

COUPLING

WALL JET		POTENTIAL FLOW
V_e along n_e	—	ϕ_n along n = b
$\frac{\partial P}{\partial s}, U_e, T_e$	—	P_b, U_b, T_b

• DIRECT PRESSURE-SPLIT COUPLING

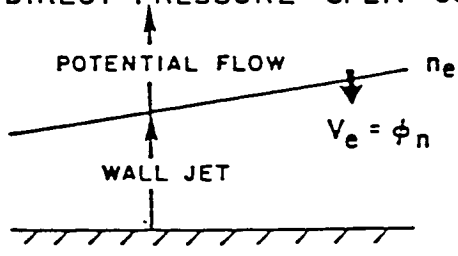

COUPLING

- As Above but Match along n_e
- P(s, n) in Jet from Normal-Momentum via Several Iterative Sweeps for Given P_e

VELOCITY-SPLIT COUPLING

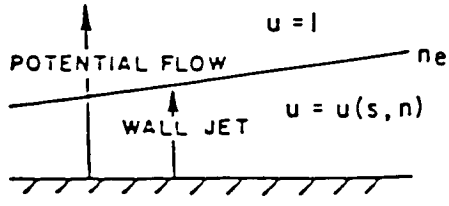

COUPLING

$U/U_E = u(1 + \phi_s)$

$V/U_E = \phi_n$

- Solutions Overlap
- Solve ϕ Equation with u(s, n) Prescribed
- Solve Wall Jet Equations with ϕ Prescribed

FIGURE 13. Coupling Procedures for Subsonic Wall Jet.

For supersonic wall jets, the viscous/inviscid coupling requirements become more complex and no coupling methodology has as yet been made operational. For supersonic free jets, the overlaid viscous/inviscid coupling approach of Dash, et.al.[39], which employs displacement-thickness coupling concepts[40] (Figure 14) has been successful in studies geared toward nozzle afterbody drag predictions[41]. The RAXJET zonal component model (which is based on this methodology) employs components (Figure 15) analogous to those utilized in the TRACON CC airfoil code. The extension of the overlaid coupling approach to wall jets was investigated by Dash[42] but found not to be a viable method (see references 4 and 5).

Recently, the direct-coupling approach for supersonic free jets has been made operational[43] utilizing a free jet version of WJET (the SPLITP model[27]) coupled to the VSAERO panel method potential solver[44]. The work (supported by AFWAL) is geared towards developing interactive methodology for VSTOL jets (Figure 16). Typical predictions are exhibited in Figures 17 and 18. Figure 17 depicts the direct-coupling boundary comprised of the nacelle surface and paneled jet boundary, $\tilde{y}_B$, which lies close to the outer jet computational boundary. Also exhibited is the source distribution, ϕ_n, applied along $\tilde{y}_B$, which combines the effects of jet entrainment (suction) and jet blockage (underexpansion - shock effects). Figure 18 depicts the predicted pressure variation along the coupling boundary $\tilde{y}_B$. In the first pass iteration, the jet is represented as a solid sting and the pressure is given by $C_p^{(1)}$. In subsequent iterations, the coupled effects of jet entrainment and blockage are evident in the pressure variation. See references 29, 43 and 45 for further details of this methodology. Progress towards using advanced coupling concepts for incorporating WJET into the TRACON CC code[12], is described in Part II of this paper[11].

ANALYSIS OF FUNDAMENTAL DATA

The data analyzed by WJET are limited to situations for which WJET can operate on a stand alone basis. Hence, the cases involve rather fundamental situations and primarily reflect upon the ability of the turbulence model incorporated in WJET. The analysis of wall jets in realistic CC airfoil flowfields requires coupling of WJET with TRACON[11]. Most of the cases analyzed have already been described in refs. 4 and 5 and only a very brief overview will be provided here.

Planar Wall Jet Issuing Into Still Air

For this simplest of all wall jet cases, the overall jet growth parameters (viz., half radius and locus of maximum velocity) predicted using the hybrid $k\varepsilon$/VanDriest turbulence model are in reasonable agreement with the data (see Figure 19), and, in better agreement than

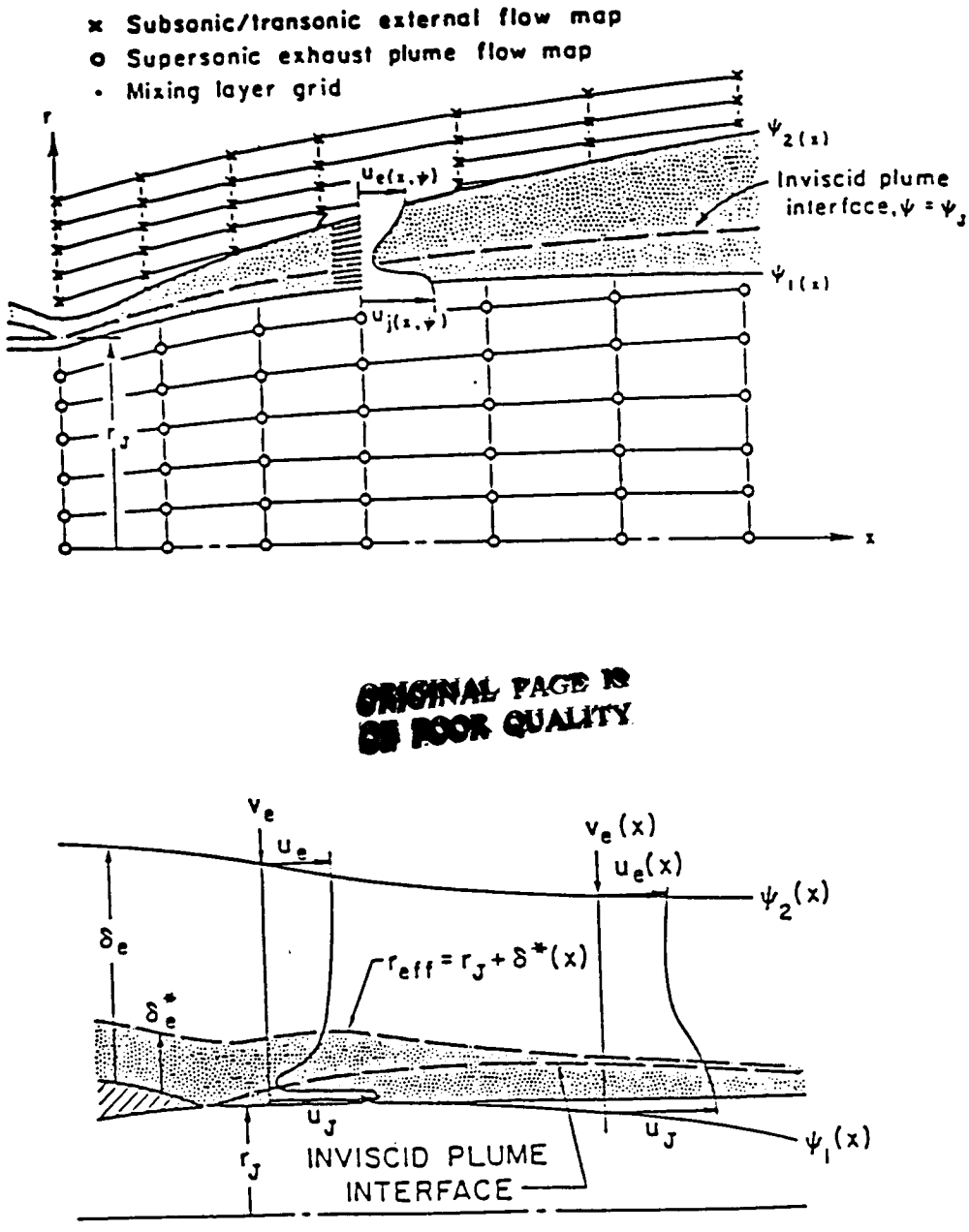

FIGURE 14. Overlaid Viscous/Inviscid Coupling Approach and Displacement-Thickness Representation of Plume Boundary.

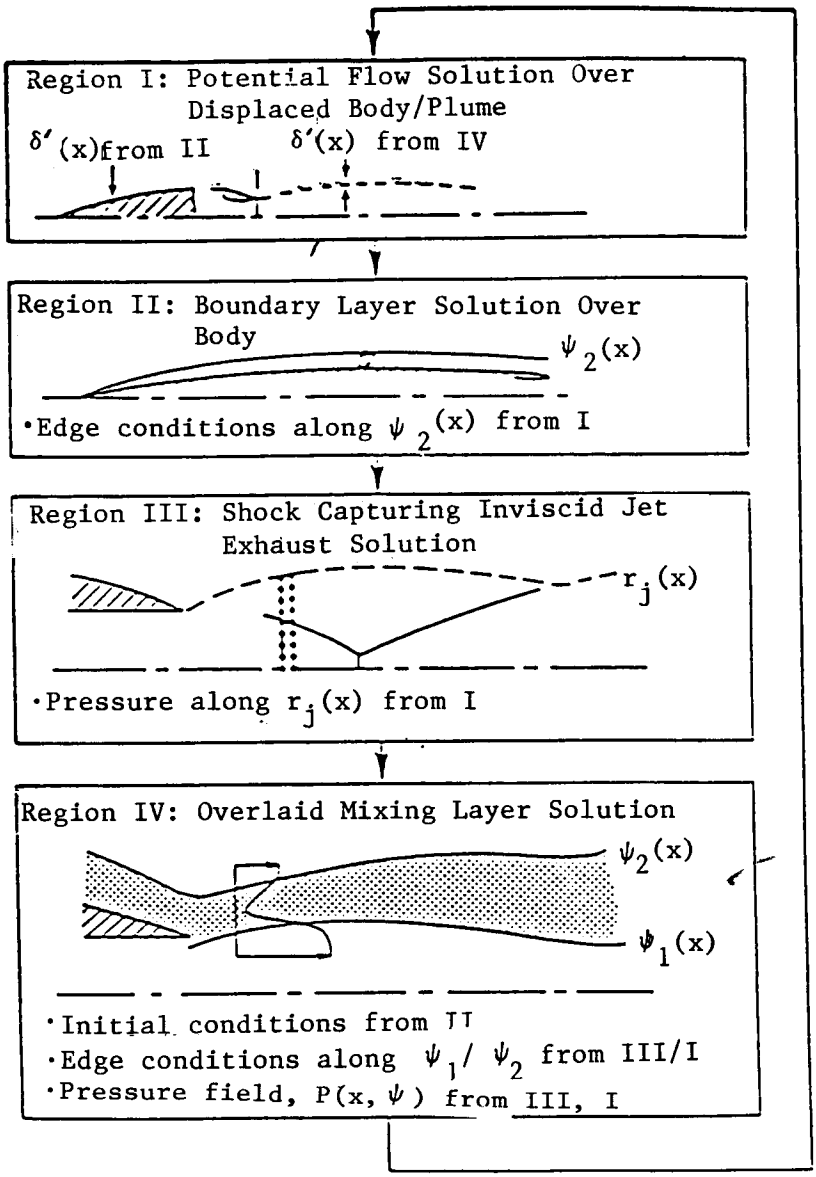

RAXJET COMPUTER MODEL (WILMOTH, NASA TM 83235, 1982)

- SOUTH/JAMESON POTENTIAL FLOW SOLVER
- INTEGRAL BL MODEL
- SCIPPY SHOCK-CAPTURING PLUME MODEL (DASH/THORPE)
- BOAT OVERLAID SHEAR LAYER SOLUTION (DASH/PERGAMENT)

FIGURE 15. **Components Utilized in RAXJET Code for Zonal Solutions of Nozzle Afterbody Drag.**

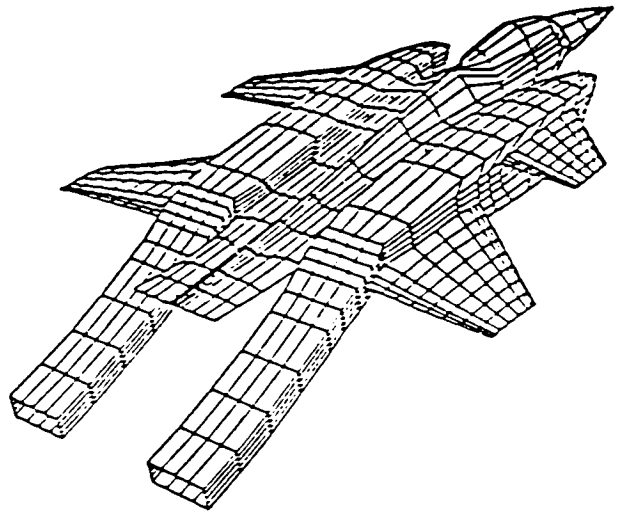

FIGURE 16. Panel Representation of STOL Fighter Model with Inclined, Rectangular Jet.

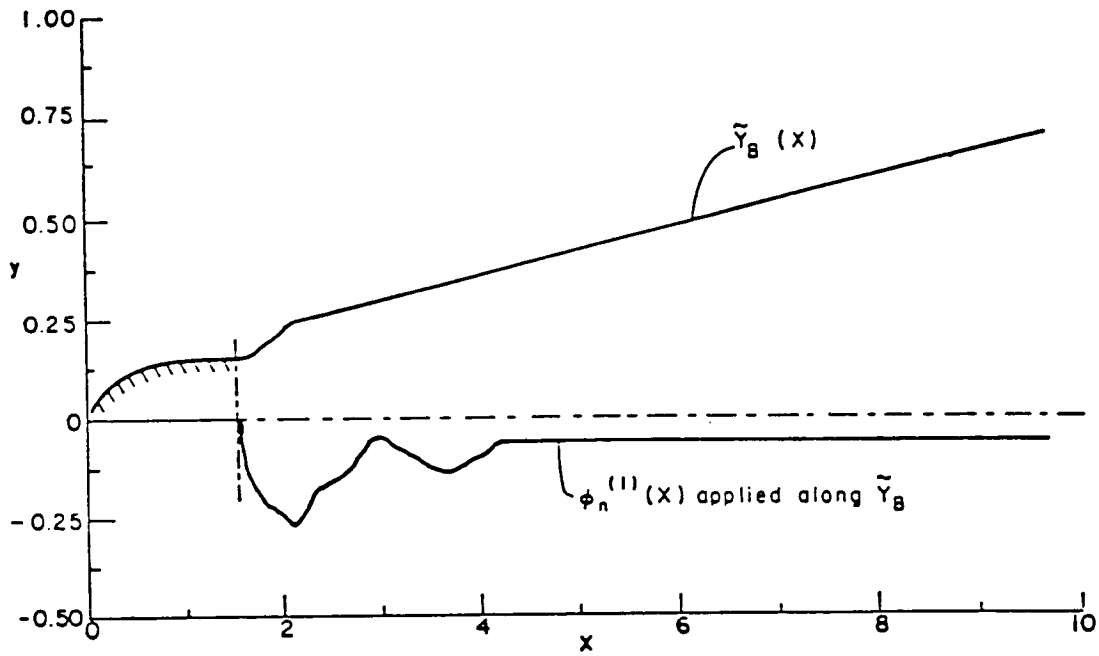

FIGURE 17. Direct-Coupling Boundary and Source Distribution.

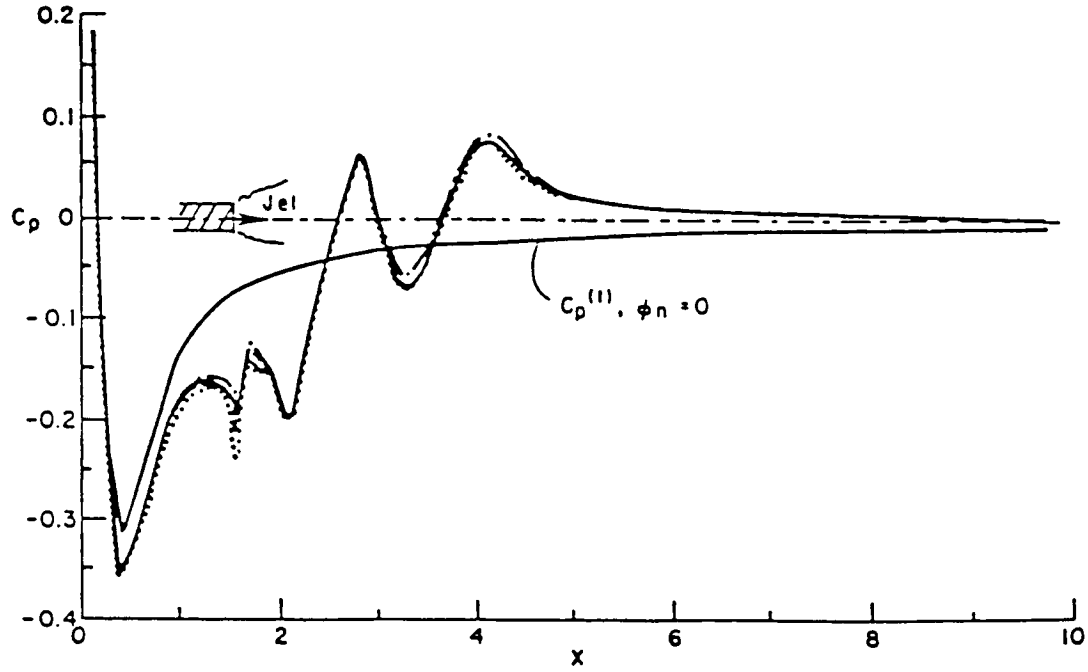

FIGURE 18. Coupling Boundary Pressure Variation for Several Shock Cells.

that of other investigators (e.g., see ref. 46) who used the $k\varepsilon$ model with a wall function near wall approximation. Also exhibited in Figure 19 is a comparison of predicted and measured maximum velocity decay with the data correlation of Rajaratnam[47]. Figure 20 compares predicted and measured[48] streamwise and normal velocity profiles at selected stations downstream of where similarity is achieved.

Planar Wall Jet with Moving Outer Stream

A number of calculations were performed[6,7] corresponding to experiments performed by Kacker and Whitelaw[49]. Figure 21 exhibits typical comparisons achieved for maximum velocity decay, half radius and maximum velocity locus variation, and wall skin friction variation. The comparisons are quite good.

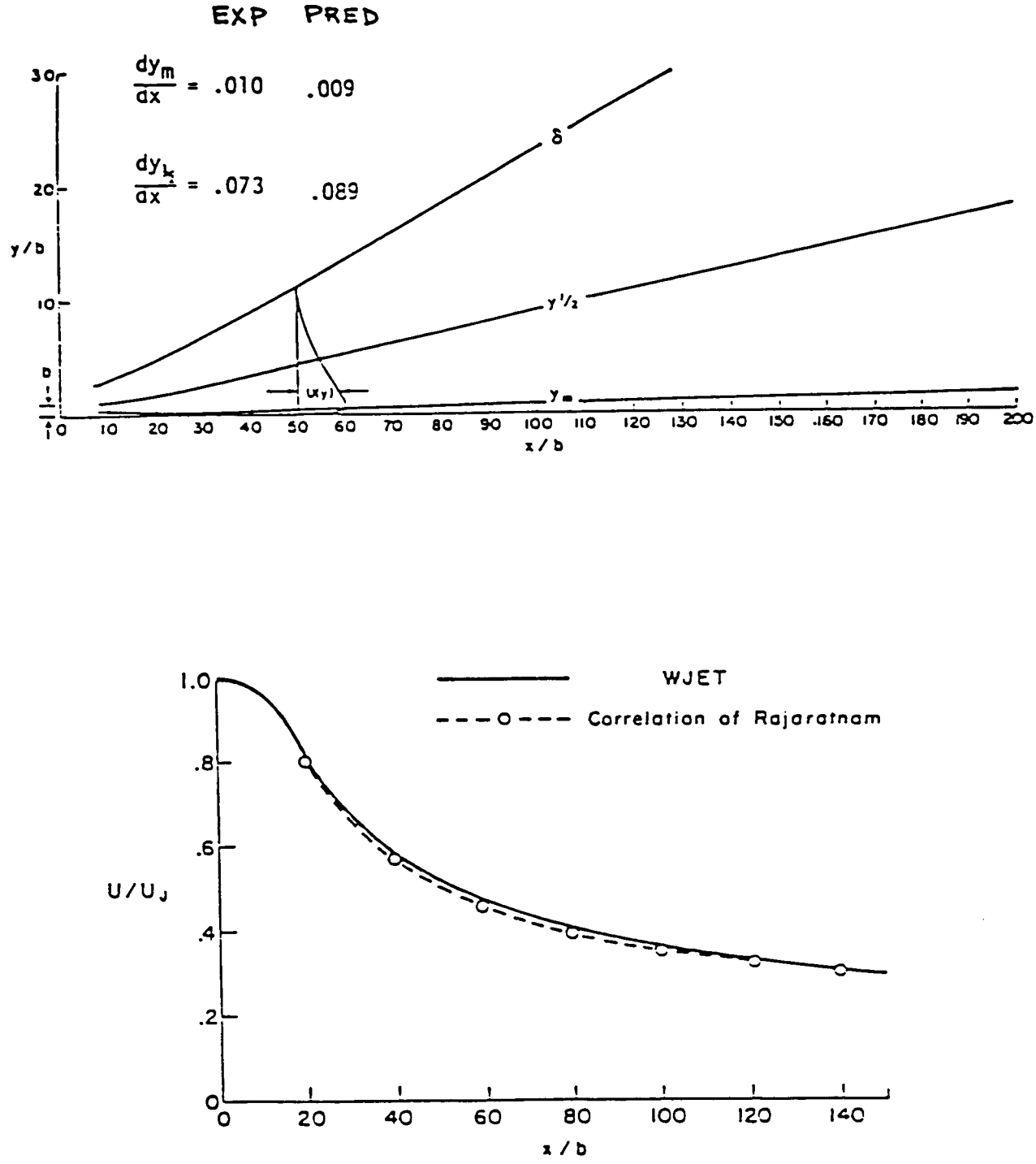

FIGURE 19. Jet Growth Parameters and Velocity Decay for Planar Wall Jet with Quiescent Outer Stream.

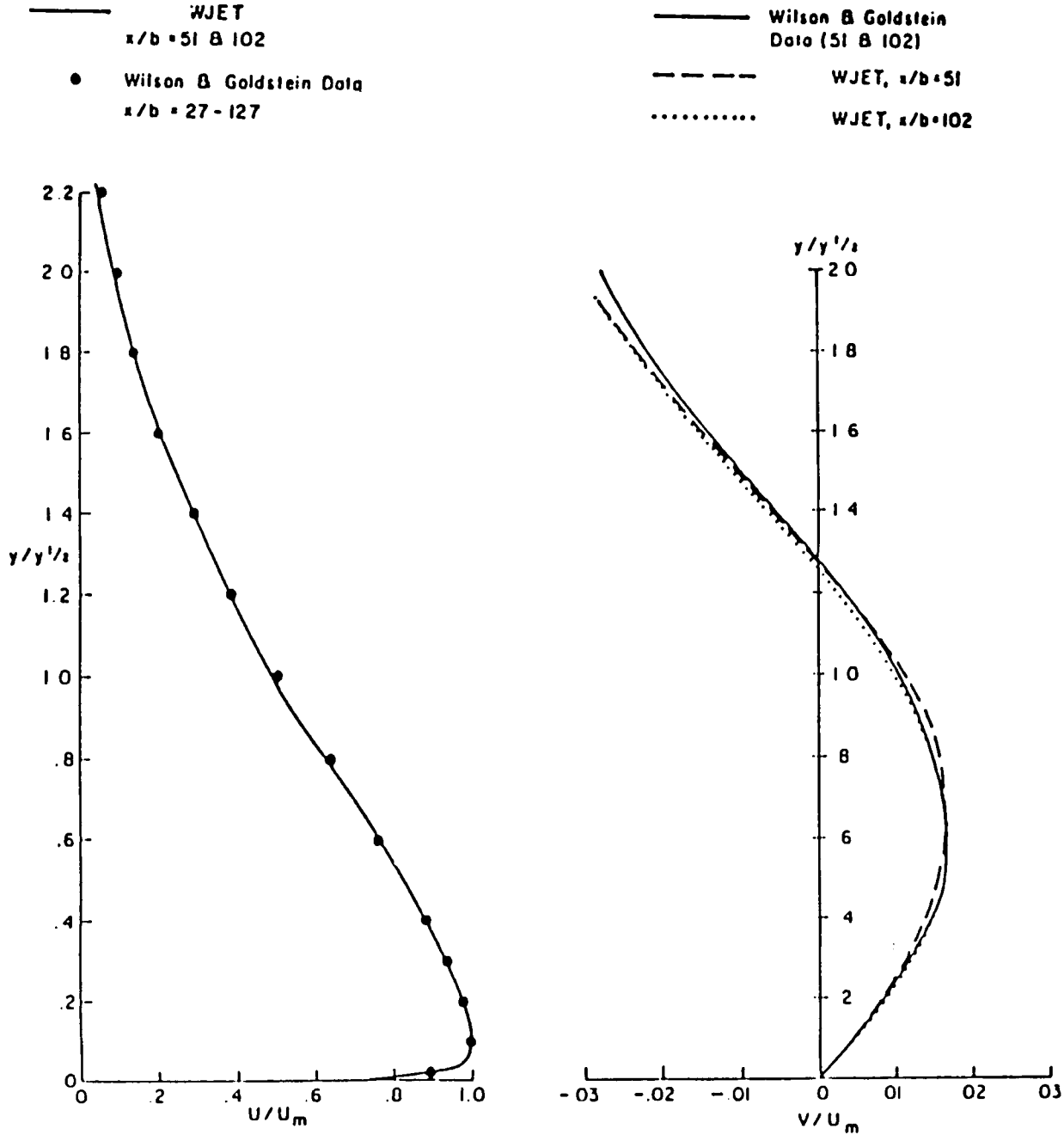

FIGURE 20. Comparison of Predicted and Measured Velocity Profiles for Planar Wall Jet with Quiescent Outer Stream.

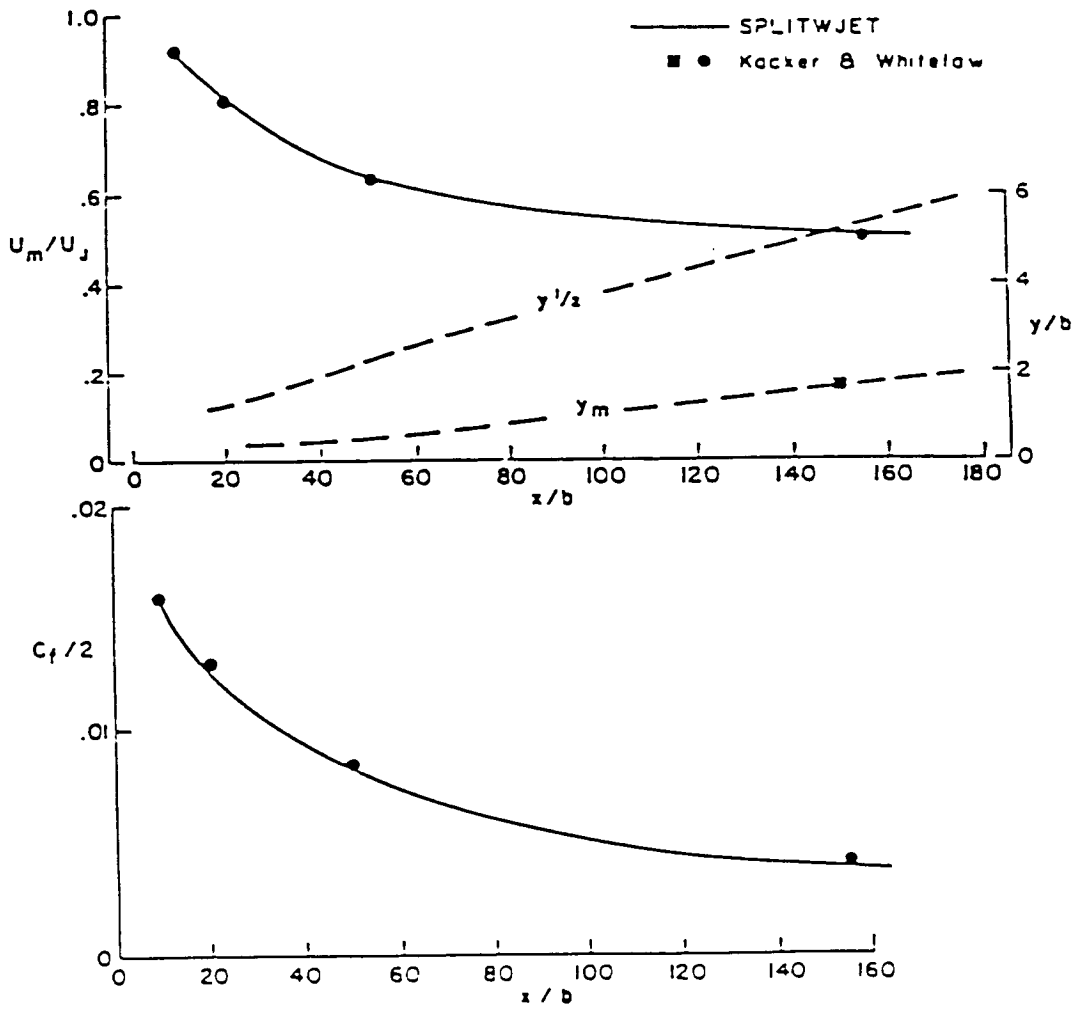

FIGURE 21. Streamwise Property Variations for Planar Wall Jet with Moving Outer Stream (U_J/U_E = 2.3).

Curved Wall Jet Issuing Into Still Air

Calculations were performed[6,7] corresponding to the experiments of Wilson and Goldstein[48]. Figure 22 depicts comparisons of half radius variation and maximum velocity decay utilizing the standard (curvilinear, s,n) $k\varepsilon$ model and versions with curvature correction terms[15,16]. The standard $k\varepsilon$-based prediction is seen to grossly underestimate the rate of mixing while curvature correction predictions (using the recommended curvature coefficient-based values of C_c = 0.2 [Launder[15]] and C_c = 0.16 [Penn State[16]]) agree quite well with the data. Profiles of turbulent shear stress performed with the two correction terms (Figure 23) agree reasonably well with each other and with the data at θ = 90°, but diverge at θ = 180°, as exhibited. Figure 24 exhibits the streamwise variation of peak turbulent shear stress and clearly exhibits the divergence in the predictions at θ = 90°. The data supports the Penn State correction, except for the abrupt jump at $\theta \sim 180°$.

Curved Wall Jet With Moving Outer Stream

The last calculation simulates one of the experiments of Kind[50], as schematized in Figure 25 - conditions correspond to the Flow II Case listed. The calculation was run using the pressure-split approach with conditions (pressure, streamwise velocity) prescribed at the jet outer edge. The predicted ΔC_p across the jet (Figure 26) is in very good agreement with the data except for $\theta > 60°$. The global pressure iteration approach was employed to eliminate the pressure-split approximation and after several iterative sweeps, significant improvement in the comparisons was obtained. The predicted variation in maximum velocity decay is exhibited in Figure 27 and the results with the curvature correction are significantly better that those with the standard $k\varepsilon$ model. The predicted variation in jet half radius is exhibited in Figure 28 and again, the improvements utilizing the curvature correction are quite significant.

CONCLUDING REMARKS

The ability to analyze fundamental wall jet data is clearly keyed to the capabilities of the turbulence model utilized. Our starting point had involved the use of a high Reynolds number two-equation $k\varepsilon$ model with heuristic corrections for streamwise curvature. This model was coupled to an inner (near wall) damped VanDriest mixing length model. Algebraic (eddy viscosity) models were not utilized since they cannot readily deal with complex jet/boundary layer length scales, with initial (slot/boundary layer) turbulence levels, and with lag effects. The curvature modifications to the ε equation[15,16], previously demonstrated to yield improvements for curved boundary layers, also appear to work quite well for curved wall jets. The use of these curvature

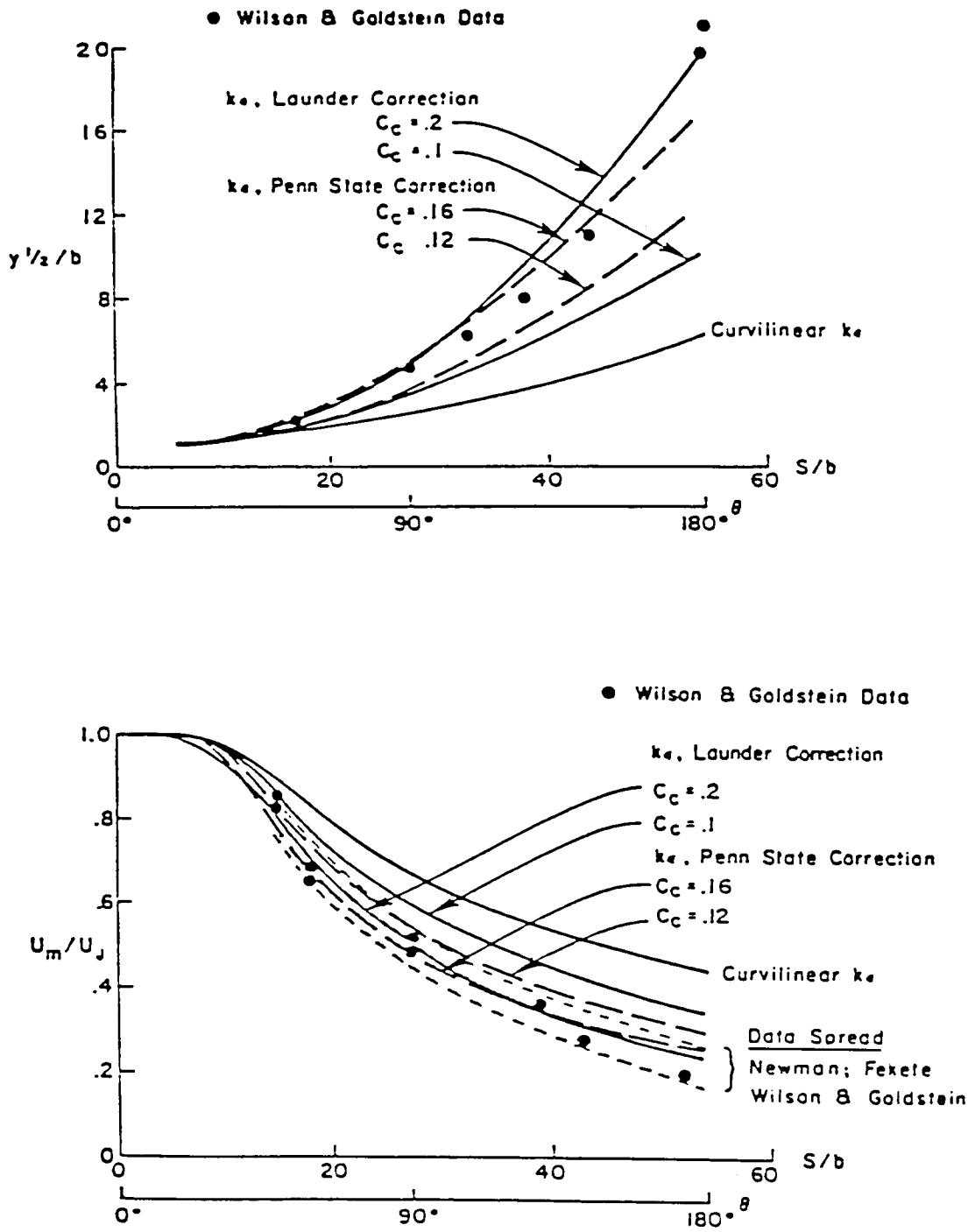

FIGURE 22. Half Radius Variation and Velocity Decay for Wall Jet Over Circular Cylinder.

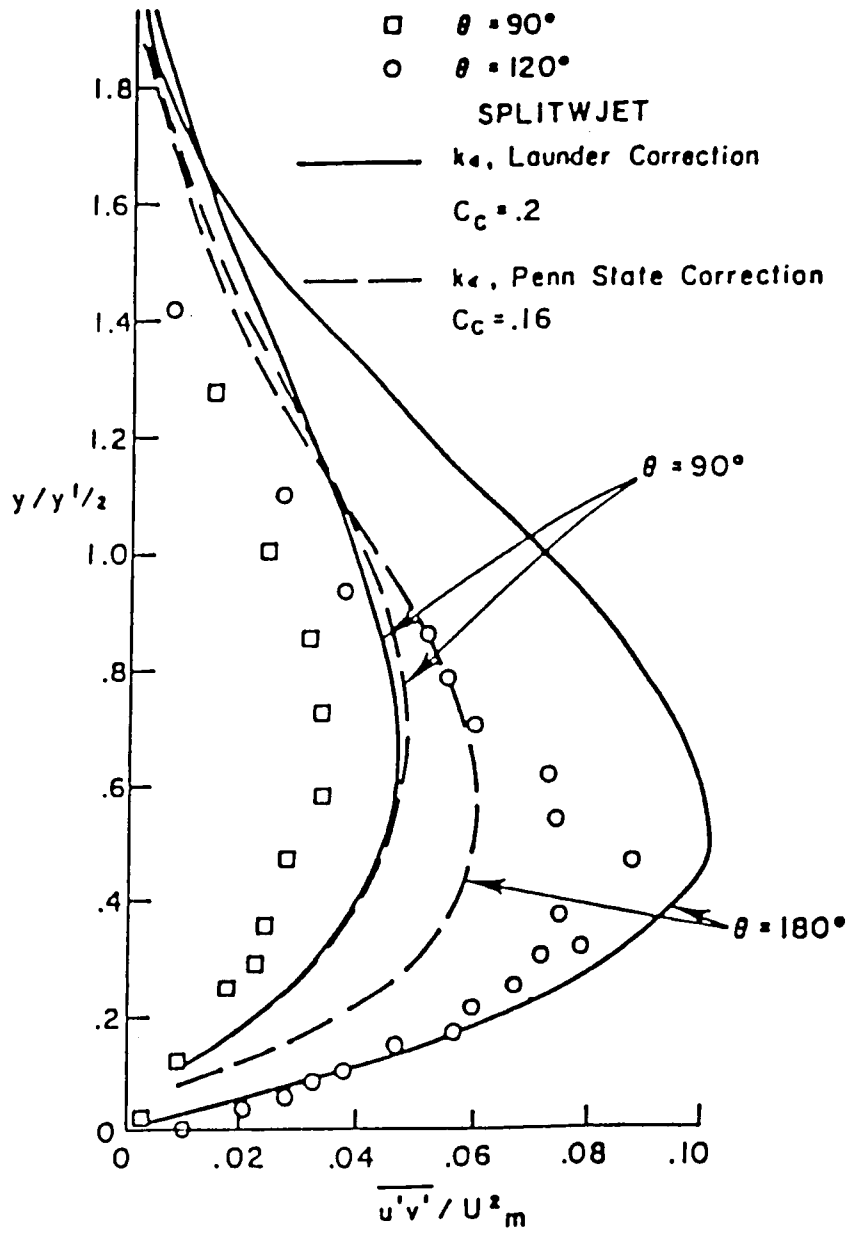

FIGURE 23. Profiles of Turbulent Shear Stress for Curved Wall Jet into Still Air.

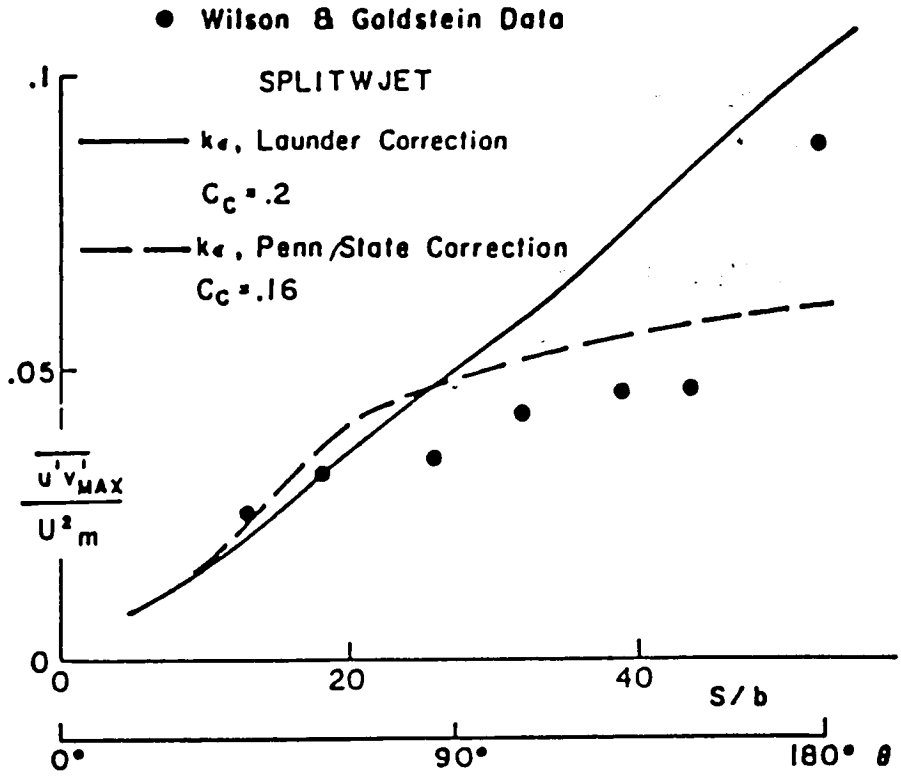

FIGURE 24. Streamwise Variation of Peak Turbulent Shear Stress for Curved Wall Jet into Still Air.

corrected models is recommended as a logical starting point for inclusion in CC NS solvers, since their ability to analyze fundamental wall jet data is reasonably well established. For supersonic wall jets, some type of compressibility correction may be required to deal with the near slot shear layer effects, but data is not presently available to support the heuristic modeling of such a correction.

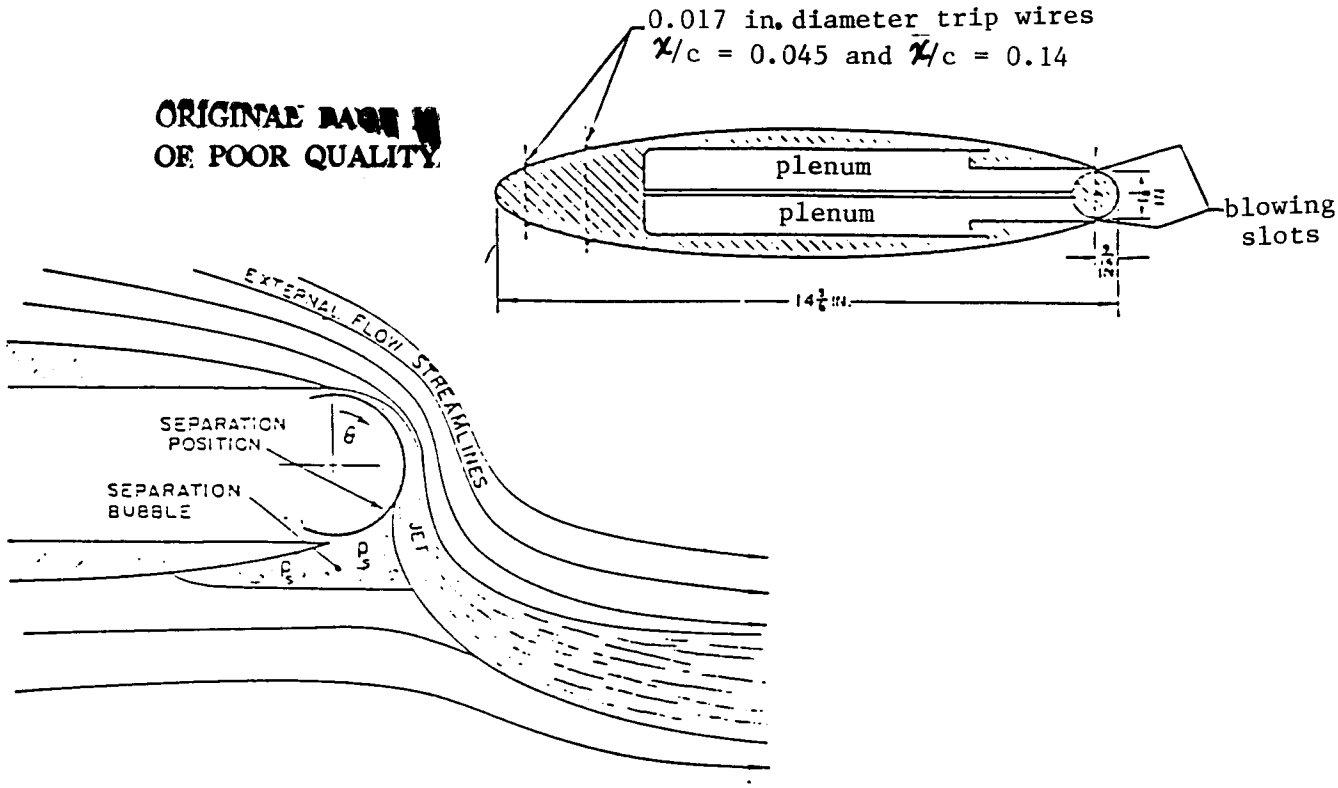

Parameters of the circulation-controlled flows for which wall-jet profile measurements were made.

	Flow I		Flow II		Flow III		Flow IV		Flow V	
C_μ	0.88		1.82		2.53		2.76		1.69	
α_{rel} (degrees)	-3.5		-0.7		+0.2		-0.8		-0.2	
C_μ	0.028		0.055		0.083		0.102		0.052	
t/c	0.0012		0.0012		0.0012		0.0012		0.0020	
U_∞ (ft/sec)	100		100		100		100		100	
R	7.5×10^5		7.5×10^5		7.5×10^5		7.5×10^5		7.5×10^5	
Surface Static Pressure Distribution	θ (deg)	$-C_{p_s}$	θ (deg)	$-C_{p_s}$	θ (deg)	$-C_{p_s}$	θ (deg)	$-C_{p_s}$	θ (deg)	$-C_{p_s}$
	0	1.54	0	2.5	0	3.54	0	4.2	0	2.25
	15	2.80	15	4.37	15	5.78	15	6.61	15	4.05
	30	3.23	30	4.88	30	6.66	30	7.81	30	4.85
	45	3.14	45	5.16	45	7.29	45	8.7	45	4.75
	60	2.39	60	4.54	60	6.63	60	8.29	60	3.95
	75	1.19	75	3.41	75	5.66	75	7.04	75	2.8
	90	-0.23	90	1.54	90	3.8	90	5.07	90	1.2
	105	-0.4	105	-0.29	105	1.4	105	2.66	105	-0.45
	120	-0.41	120	-0.58	120	-0.53	120	-0.26	120	-0.57
	135	-0.43	135	-0.63	135	-0.76	135	-0.77	135	-0.59
	150	-0.40	150	-0.64	150	-0.81	150	-0.86	150	-0.58

FIGURE 25. Kind CC Airfoil Experiment.

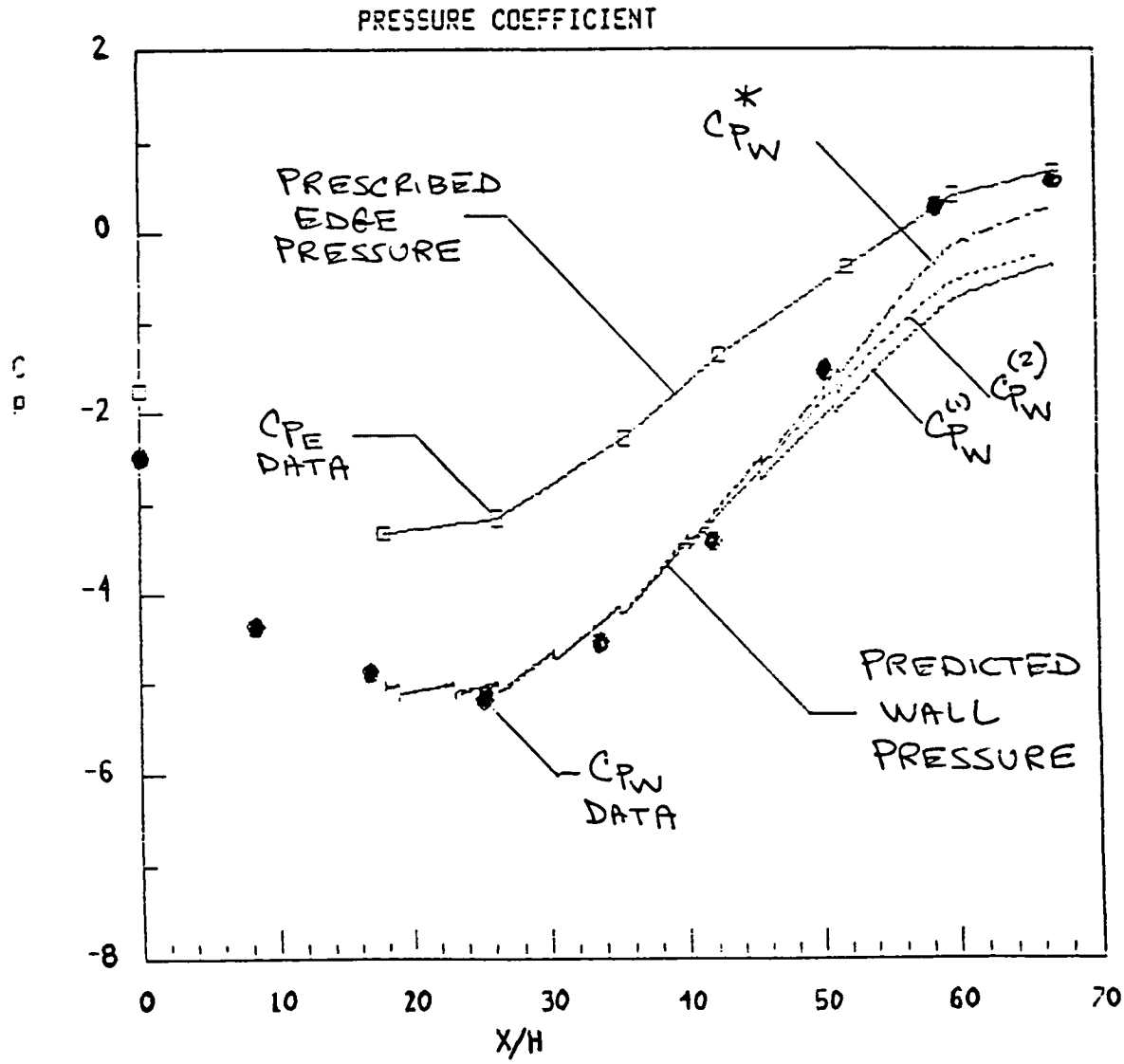

FIGURE 26. Prediction of ΔC_p Across Wall Jet for Kind CC Airfoil Problem.

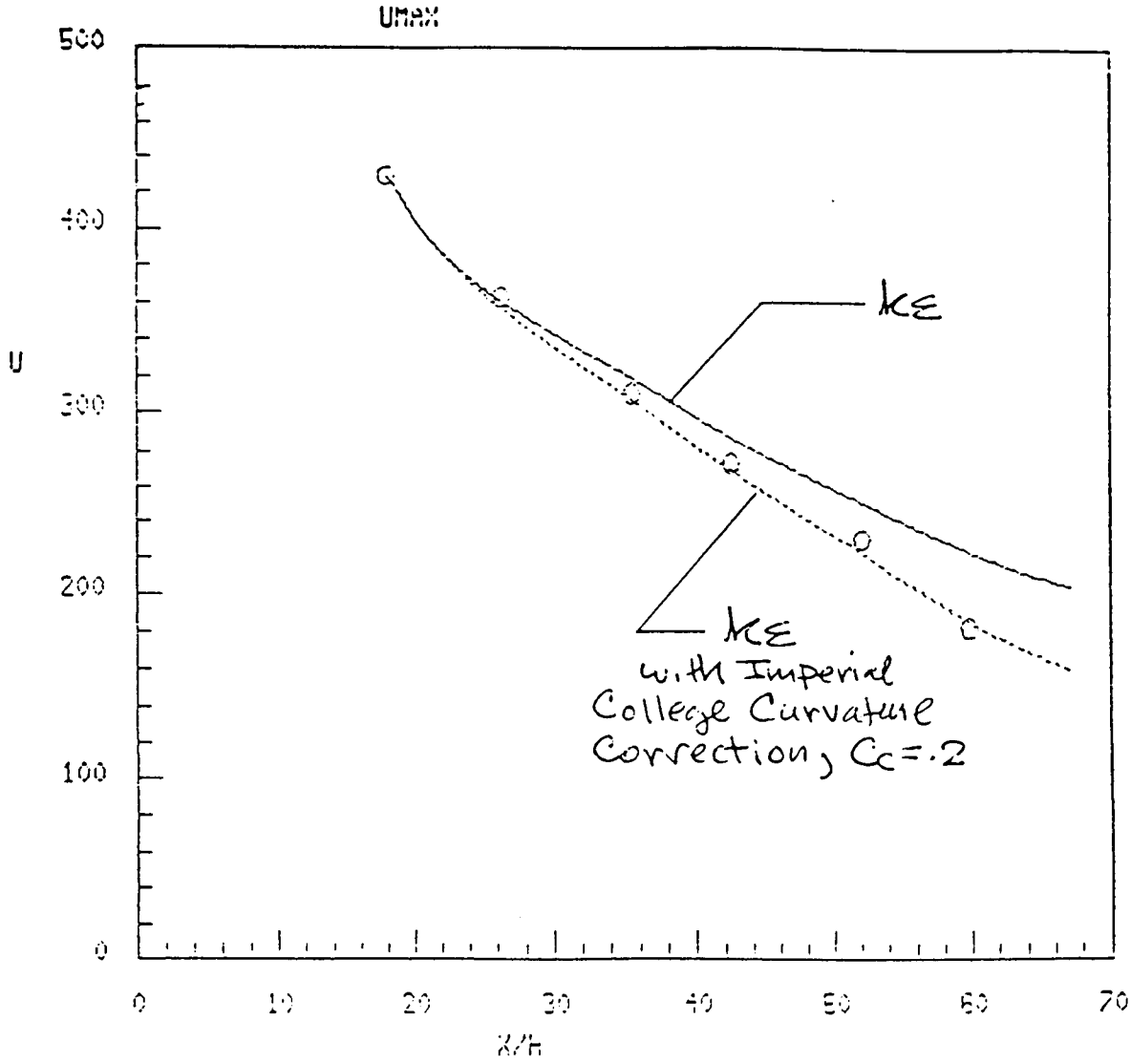

FIGURE 27. Prediction of Maximum Velocity Decay for Kind CC Airfoil Problem.

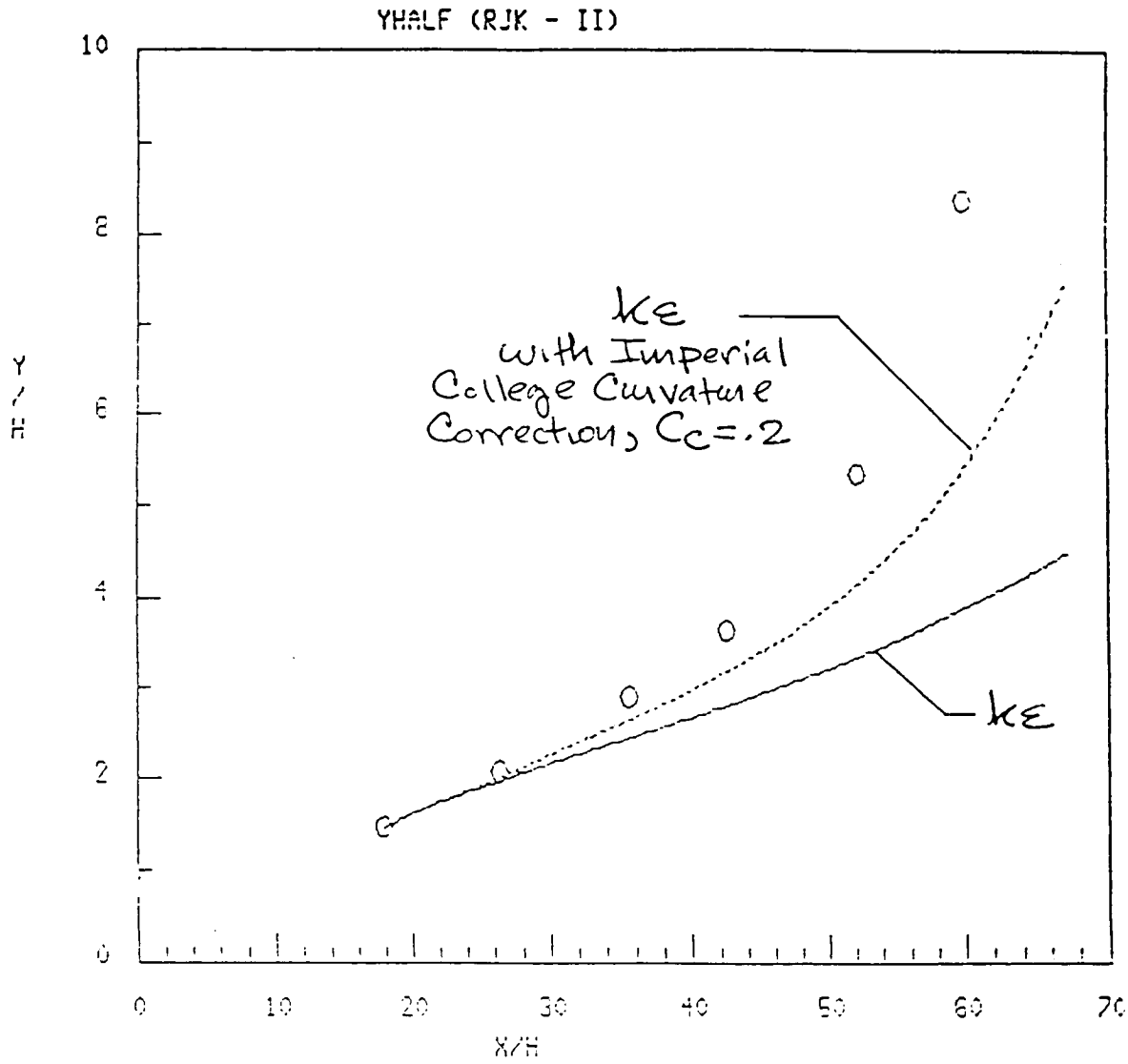

FIGURE 28. Prediction of Jet Half Radius Variation for Kind CC Airfoil Problem.

REFERENCES

1. Dvorak, F.A. and Choi, D.H., 'Analysis of Circulation-Controlled Airfoils in Transonic Flow', J. Aircraft, Vol. 20, April 1983.

2. Dvorak, F.A. and Choi, D.H., 'Development of an Analytical Method for Two-Dimensional Circulation-Control Airfoils in Transonic Flow', Analytical Methods, Inc., Redmond, WA, Report 8106, June 1981.

3. Dvorak, F.A., Calculation of Turbulent Boundary Layers and Wall Jets Over Curved Surfaces', AIAA J., Vol. 11, April 1973.

4. Dash, S.M., Beddini, R.A., Wolf, D.E. and Sinha, N., 'Viscous/ Inviscid Analysis of Curved Sub- or Supersonic Wall Jets', AIAA J., Vol. 23, January 1985, pp. 12-13.

5. Dash, S.M. and Beddini, R.A., 'Viscous/Inviscid Analysis of Curved Wall Jets: Part 2 - Viscous Pressure-Split Model (SPLITWJET)', Science Applications, Inc., Princeton, NJ, SAI/PR TR-7, November 1982.

6. Dash, S.M. and Sinha, N., 'Noniterative Cross-Flow Integration for the Pressure-Split Analysis of Subsonic Mixing Layer Problems', AIAA J., Vol. 23, January 1985, pp. 183-185.

7. Dash, S.M. and Sinha, N., 'Pressure-Split Extensions of SPLITWJET Model for Wall Jet/Potential Flow Coupling', Science Applications, Inc., Princeton, NJ, SAI/PR TR-17, February 1984.

8. Dash, S.M., Sinha, N. and York, B.J., 'Implicit/Explicit Analysis of Interactive Phenomena in Supersonic, Chemically-Reacting, Mixing and Boundary Layer Problems', AIAA Paper 85-1717, Cincinnati, OH, July 1985.

9. Dash, S.M. and York, B.J., 'Analysis of Curved, Underexpanded Wall Jets Using an Implicit/Explicit Parabolized Navier-Stokes Approach', Science Applications International Corporation, Princeton, NJ, SAIC/PR TR-29, June 1985.

10. Dvorak, F.A. and Dash, S.M., 'Improved Algorithms for Analysis of Circulation Control Rotors' Analytical Methods, Inc., Redmond, WA, Report No. 8407, May 1984.

11. Dvorak, F.A. and Dash, S.M., 'Wall Jet Analysis for Circulation Control Aerodynamics; Part II - Zonal Modeling Concepts for Wall Jet/Potential Flow Coupling', Circulation Control Workshop, NASA Ames Reserach Center, Moffett Field, CA, Feb. 18-20, 1985.

12. Arora, R., Kuo, K.K., and Razdan, M.K., 'Near Wall Treatment for Turbulent Boundary Layer Computations,' AIAA J., Nov. 1982. pp. 1481-2.

13. Bradshaw, P., 'The Analogy Between Streamline Curvature and Buoyancy in Turbulent Shear Flow', J. Fluid Mech., 36, 1969, pp. 177-191.

14. Foloyan, C.O. and Whitelaw, J.H., 'The Effectiveness of Two-Dimensional Film Cooling Over Curved Surfaces', ASME Paper 76-HT-31, 1976.

15. Launder, B.E., Priddin, C.H. and Sharma, B.I., 'The Calculation of Turbulent Boundary Layers on Spinning and Curved Surfaces,' ASME J. Fluids Eng., March 1977, pp. 231-239.

16. Hah, C. and Lakshminarayana, B., 'Prediction of Two- and Three-Dimensional Axisymmetric Turbulent Wakes, Including Curvature and Rotation Effects', AIAA J., Oct. 1980, pp. 1196-1204.

17. Dash, S.M., Weilerstein, G. and Vaglio-Laurin, R., 'Compressibility Effects in Free Turbulent Shear Flows', Air Force Office of Scientific Research, TR-75-1436, August 1975.

18. Mahgoub, H.E.H. and Bradshaw, P., 'Calculation of Turbulent-Inviscid Flow Interactions with Large Normal Pressure Gradients', AIAA Journal, October 1979, pp. 1025-1029.

19. Chen, Z.B. and Bradshaw, P., 'Calculation of Viscous Transonic Flow over Airfoils', AIAA J., February 1984, pp. 201-205 (also, AIAA Paper 82-0997, June 1982).

20. Moretti, G., 'Analysis of Two-Dimensional Problems of Supersonic Combustion Controlled by Mixing,' AIAA J., Vol. 3, 1965, pp. 223-229, (also AIAA Paper 64-96, Jan. 1964).

21. Ferri, A. and Dash, S.M., 'Viscous Flow at High Mach Numbers with Pressure Gradients', Viscous Interaction Phenomena in Supersonic and Hypersonic Flow, University of Dayton Press, Dayton, OH, 1970, pp. 271-318.

22. Sinha, N. and Dash, S.M., 'Parabolized Navier-Stokes Analysis of Ducted Turbulent Mixing Problems with Finite-Rate Chemistry,' AIAA Paper 86-0004, January 1976.

23. Dash, S.M. and Wolf, D.E., 'Fully-Coupled Analysis of Jet Mixing Problems, Part I: Shock-Capturing Model, SCIPVIS', NASA CR-3761, January 1984.

24. Dash, S.M. and Wolf, D.E., 'Interactive Phenomena in Supersonic Jet Mixing Problems, Part I: Phenomenology and Numerical Modeling Techniques', AIAA J., Vol. 22, July 1984, pp. 905-913.

25. Dash, S.M. and Wolf, D.E., 'Interactive Phenomena in Supersonic Jet Mixing Problems, Part II: Numerical Studies', AIAA J., Vol. 22, October 1984, pp. 1395-1404.

26. Dash, S.M., Wolf, D.E. and Seiner, J.M., 'Analysis of Turbulent Underexpanded Jets - Part I: Parabolized Navier-Stokes Model, SCIPVIS', AIAA J., Vol. 23, April 1985, pp. 505-514.

27. Dash, S.M. and Sinha, N., 'Fully-Coupled Analysis of Jet Mixing Problems, Part II: Pressure-Split Model, SPLITP', NASA CR in preparation.

28. Seiner, J.M., Dash, S.M. and Wolf, D.E., 'Analysis of Turbulent Underexpanded Jets - Part II: Shock Noise Features Using SCIPVIS', AIAA J., Vol. 23, May 1985.

29. Dash, S.M., 'Recent Developments in the Modeling of High Speed Jets, Plumes and Wakes - Invited Survey Paper', AIAA Paper 85-1616, Cincinnati, OH, July 1985.

30. Pergament, H.S., Dash, S.M. and Varma, A.K., 'Evaluation of Turbulence Model for Rocket and Aircraft Plume Flowfield Predictions', AIAA Paper 79-0359, New Orleans, LA, January 1979.

31. Pergament, H.S., 'Assessment and Recommendation of Two-Equation Turbulence Models for Rocket and Aircraft Plume Flowfield Predictions', Naval Weapons Center, China Lake, CA, TP 6364, July 1982.

32. Pergament, H.S., Sinha, N. and Dash, S.M., 'Hybrid Two-Equation Model for High Speed Propulsive Jets', to be presented at AIAA/ASME Joint Propulsion Conference, Huntsville, AL, June 1986.

33. Langanelli, A.L. and Leone, S.A., 'Inclined Slot Jet Evaluation Progress Report', Science Applications International Corporation, Valley Forge, PA, January 1986.

34. Dash, S.M., 'Compressibility Effects in High Mach Number Turbulent Mixing Problems', Science Applications International Corporation, Princeton, NJ, TL-234, August 1985.

35. Dodge, P.R., 'A Numerical Method for 2D and 3D Viscous Flows', AIAA J., July 1977, pp. 961-965 (also AIAA Paper 76-425, July 1976).

36. Khosla, P.K. and Rubin, S.G., 'A Composite Velocity Procedure for the Compressible Navier-Stokes Equations', AIAA Paper 82-0099, Jan. 1982.

37. Cosner, R.R., 'Fast Navier-Stokes Solution of Transonic Flowfield About Axisymmetric Afterbodies', AIAA Paper 80-0193, Jan. 1980.

38. Swanson, R.C., Rubin, S.G. and Khosla, P.K., 'Calculation of Afterbody Flows with a Composite Velocity Formulation', AIAA Paper 83-1736, July 1983.

39. Dash, S.M., Wilmoth, R.G. and Pergament, H.S., 'An Overlaid Viscous/Inviscid Model for the Prediction of Nearfield Jet Entrainment', AIAA J., Vol. 17, September 1979, pp. 950-958.

40. Wilmoth, R.G. and Dash, S.M., 'A Viscous-Inviscid Interaction Model of Jet Entrainment', Computation of Viscous-Inviscid Interactions, AGARD CP-291, September 1980, pp. 13.1 - 13.15.

41. Wilmoth, R.G., 'RAXJET: A Computer Program for Predicting Transonic Axisymmetric Flow Over Nozzle Afterbodies with Supersonic Jet Exhaust', NASA TM 83235, Feb. 1982.

42. Dash, S.M., 'An Overlaid Procedure for the Viscous/Inviscid Analysis of Wall Jets', Science Applications, Inc., Princeton, NJ, SAI/PR TM-2, December 1980.

43. Dash, S.M. and Lee, S.H., 'Exploratory Investigation of Jet/Potential Flow Coupling Using SPLITP Jet and VSAERO Panel Codes', Science Applications International Corporation, Princeton, NJ, SAIC/PR TM-39, April 1985.

44. Maskew, B., 'Program VSAERO: A Computer Program for Calculating the Non-Linear Aerodynamic Characteristics of Arbitrary Configurations', NASA CR-166476, December 1982.

45. Dash, S.M., Wolf, D.E., Sinha, N. and Lee, S.H., 'Progress in the Development of Parabolized Navier-Stokes Methodology for Analyzing 3D Propulsive Jet Flowfields', AIAA Paper 86-1115, AIAA/ASME 4th Fluid and Plasma Dynamics Meeting, Atlanta, GA, May 1986.

46. Ljuboja, M. and Rodi, W., 'Calculation of Turbulent Wall Jets with an Algebraic Reynolds Stress Model', ASME J. Fluids Eng., Sept. 1980, pp. 350-356.

47. Rajaratnam, N., Turbulent Jets, Elsavier, Amsterdam, The Netherlands, 1976, Chapter 10.

48. Wilson, D.J. and Goldstein, R.J., 'Turbulent Wall Jets with Cylindrical Streamwise Surface Curvature', ASME J. Fluids Eng., Sept. 1976, p. 550-557.

49. Kacker, S.C. and Whitelaw, J.H., 'The Turbulent Characteristics of Two-Dimensional Wall-Jet and Wall-Wake Flows', ASME J. App. Mech., March 1971, pp. 239-252.

50. Kind, R.J., 'A Calculation Method for Circulation Control by Tangential Blowing Around a Bluff Trailing Edge', Aeronautical Quarterly, August 1968, pp. 205-223.